DOI: 10.1002/chem.201001721

Imidazoliophosphines are True N-Heterocyclic Carbene (NHC)–Phosphenium Adducts

Ibrahim Abdellah,[a, b] Christine Lepetit,[a, b] Yves Canac,*[a, b] Carine Duhayon,[a, b] and Remi Chauvin*[a, b]

Abstract: Whereas the external nucleophilic reactivity of α-amidiniophosphines has been previously illustrated by their complexation to transition-metal centers, their internal electrophilic reactivity is herein investigated by using BIMIONAP (BIMIONAP = N-methylated BIMINAP cation, BIMINAP = formal contraction of the acronyms BIMIP = 2,2′-bis(diphenylphosphino)-1,1′-bibenzimidazole and BINAP = 2,2′-bis(diphenylphosphino)-1,1′-binaphthyl). Reaction of tetraethylammonium chloride with free BIMIONAP is found to induce heterolytic cleavage of the N_2C–P bond to give chlorodiphenylphosphine and a transient phosphine–N-heterocyclic carbene (NHC) species that is trapped in situ by protonation to the corresponding phosphine–benzimidazolium cation. When the chloride anion reacts with the cationic [Pd(η^2-BIMIONAP)Cl_2] complex, the same cleavage occurs and the phosphine–NHC moiety is trapped in the corresponding [$PdCl_2$(η^2-phosphine–NHC)] complex. When the chloride anion reacts with the dicationic [Pd(π-allyl)(η^2-BIMIONAP)]$^+$ complex, allyldiphenylphosphine is produced, and the [PdCl(η^2-phosphine–NHC)($PPh_2CH_2CH{=}CH_2$)]$^+$ complex is obtained. Reaction of free BIMIONAP with the harder *n*-butyllithium nucleophile also induces heterolytic cleavage of the N_2C–P bond, from which the phosphine–NHC moiety is trapped by hydrolysis of the benzimidazole ring or by P,C-sulfurization. Cleavage of a C–P bond with the weak Cl^- nucleophile to release the reactive NHC moiety (according to the unusual scheme C–P + Cl^- → C: + Cl–P) is a definite experimental indication of the dative nature of the N_2C–P bond of amidiniophosphines, which are, therefore, better described as NHC→phosphenium adducts. This interpretation is supported by the calculation, at the DFT level, of a heterolytic dissociation mode of the N_2C–P bond lower in energy than the homolytic one. A mesomeric description of the NHC→phosphenium entity is also proposed on the basis of electron localization function (ELF) and atoms in molecules (AIM) analyses. Finally ELF and AIM-based Fukui indices, molecular orbitals, and MESP analyses show that the initial attack of Cl^- takes place at the carbenic atom of BIMIONAP.

Keywords: dative bonding · electrostatic interactions · N-heterocyclic carbenes · palladium · phosphenium

Introduction

In current chemical drawing, the dative symbol D→A is formally equivalent to the α-zwitterionic Lewis symbol D^+–A^-, for which the dash "–" denotes a shared electron pair. Nevertheless, the D→A symbol features more than topological information, and should be reserved for demonstrated relevant cases. Indeed, the dative nature of a covalent bond A–B is determined by an energetical criterion, namely, by its preference for a heterolytic dissociation mode A–B→A^+ + $|B^-$ versus the corresponding homolytic mode A–B→ $A^\bullet$ + $B^\bullet$.[1] The difference in energy between the two modes of dissociation is $\Delta D = IP(A^\bullet) - EA(B^\bullet)$, in which *IP* and *EA* denote the ionization potential and the electron affinity, respectively. If $A^\bullet$ and $B^\bullet$ are neutral, the homolytic rupture is

[a] I. Abdellah, Dr. C. Lepetit, Dr. Y. Canac, C. Duhayon, Prof. R. Chauvin
CNRS, LCC (Laboratoire de Chimie de Coordination)
205, route de Narbonne, 31077 Toulouse (France)
Fax: (+33) 561-553-003
E-mail: yves.canac@lcc-toulouse.fr
chauvin@lcc-toulouse.fr

[b] I. Abdellah, Dr. C. Lepetit, Dr. Y. Canac, C. Duhayon, Prof. R. Chauvin
Université de Toulouse, UPS, INP, LCC
31077 Toulouse (France)

Supporting information for this article is available on the WWW under http://dx.doi.org/10.1002/chem.201001721.

generally favored because of the destabilizing electrostatic term of the heterolytic rupture (for neutral species indeed, $IP \gg EA$ in order of magnitude). If A$^{\bullet}$ or B$^{\bullet}$ is charged (e.g. if B$^{\bullet}$ is a cation), the heterolytic dissociation leads to at least one neutral closed-shell species, and is thus a priori lower in energy due to the vanishing of the electrostatic term. Although the minimum-energy dissociation mode in the gas phase can be investigated by DFT or ab initio calculations, experimental indications are provided by intrinsic structural features of the bond: high polarity, great length, and low strength. In particular, the low strength of an A–B dative bond and the accepting character of the A moiety are experimentally revealed by the displacement of an intrinsically reactive B entity with a relatively stable B′ counterpart.[2] This kind of reactivity defines the field of coordination chemistry, in which the acceptor component A (a Lewis acid) is a metallic center M, and the donor component (a Lewis base) is a neutral ligand L. Assignment of the donor–acceptor character may, however, require refining when M and L are amphoteric and the M–L interaction is not a pure simple covalent bond, that is, it involves more than two electrons. The coordination of carbonyl and corresponding Fisher carbenes are paradigms of this situation. In contrast, diaminals thereof, namely cyclic diamino-carbenes (N-heterocyclic carbenes (NHCs)), are currently recognized as pure two-electron donating neutral ligands,[3] but selective displacement of coordinated NHCs from transition-metal centers by other nucleophiles has not been exemplified to the best of our knowledge: experimental evidence of the dative nature of the NHC→M bond is thus missing. However, NHCs may also be regarded as "stabilizing ligands" of highly reactive nonmetallic electrodeficient species with low coordinence. Stabilization of p-block elements in the zero-oxidation state by NHCs was recently reported for the :Si=Si:,[4] :Ge=Ge:,[5] :P–P:,[6] P_n,[7] and C_1 fragments.[8] Additionally, various oxidation states encountered in germylenes Ge^{II},[9] silylenes Si^{II},[10] borenium B^{III},[11] or tellerium Te^{II}[12] cations have also been reported to be efficiently stabilized by NHC ligands. By extension, even tetraaminoethenes could be interpreted as the ultimate products of primary donor–acceptor adducts between the filled sp^2 orbital of one diaminocarbene and the formally empty p orbital of the other.[13]

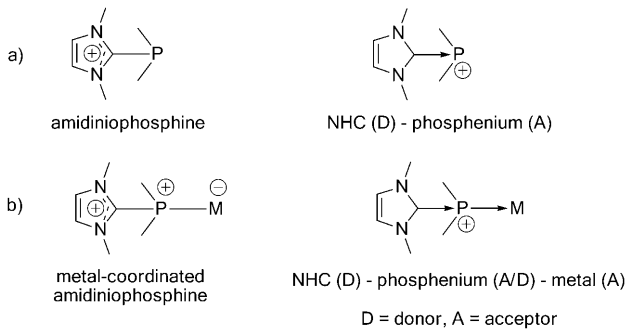

Scheme 1. Lewis representation of amidiniophosphines (left) versus dative representation of the corresponding NHC–phosphoniums (right): a) in the free state; b) in the metal–P-coordinated state.

In the cationic series, phosphoniums $R_2P{:}^+$, which are isolobal and isovalent of singlet carbenes, formally contain a sp^2-hybridized P^{III} atom with a lone pair of electrons in a σ-type orbital and an empty p_π-type orbital. Their Lewis amphoteric character make them ideal candidates to act simultaneously as acceptors and as donors (Scheme 1a). Beyond the stable free diaminophospheniums,[14] phosphenium cations with alkyl and aryl substituents have been a priori regarded as "D→phosphenium adducts" with different donor groups D, such as phosphines, amines, or carbenes.[15] In the phosphine–phosphenium series, the dative nature of the interaction has been demonstrated by the reactivity criterion, namely, by facile ligand exchange at the phosphenium center.[16] In the NHC–phosphenium series, few theoretical studies in the gas phase[17] and X-ray diffraction analysis in the crystal state[18] supported the relevance of this appellation. Any convincing reactivity result is, however, missing, and the same cations were more prudently designated by other authors as "amidiniophosphines" with the formula $Im^+–R_2P$ instead of $N_2C→PR_2^+$ (in which Im^+ denotes a *N*-aryl,*N*′-alkyl-imidazolio substituent, Scheme 1a). The same questions apply in the metal–P-coordinated series (Scheme 1b).[19]

Following pioneering reports of monodentate amidiniophosphine ligands,[20] we recently described the BIMIONAP (BIMIONAP = N-methylated BIMINAP cation, BIMINAP = formal contraction of the acronyms BIMIP = 2,2′-bis(diphenylphosphino)-1,1′-bibenzimidazole and BINAP = 2,2′-bis(diphenylphosphino)-1,1′-binaphthyl) chelate version **1**, combining an amidiniophosphine end with a neutral phosphine end.[18a] In the palladium series, BIMIONAP was shown to act as a *cis*-chelating ligand in a seven-membered metallacycle. It was observed that this cationic ligand is much less electron-donating than the BIMINAP neutral analogue and exhibits specific catalytic properties.[18a] In the following report, the nature of the $N_2C–PR_2$ bond of BIMIONAP is investigated through both the reactivity criterion by using the chloride ion as a relatively "stable " nucleophile (relative to NHC) and theoretical analyses by using the electron localization function (ELF).

Results and Discussion

Displacement of a NHC unit from the free phosphenium end of BIMIONAP (**1**) by a chloride ion is expected to afford chlorodiphenylphosphine (Ph_2PCl), which can be easily identified by ^{31}P NMR spectroscopy. The relevance of such a transformation in the field of coordination chemistry is a priori supported by evidence for the dative character of P–halogen bonds.[2d–e] The concommitent generation of the highly reactive free NHC unit could be indicated by the final presence of the corresponding iminium resulting from hydrolysis (Scheme 2a). Hydrolytic trapping is, however, difficult to control in two steps and evidence of the putative transient NHC is thus also sought for by an intramolecular trapping strategy from palladium(II) complexes of BIMIO-

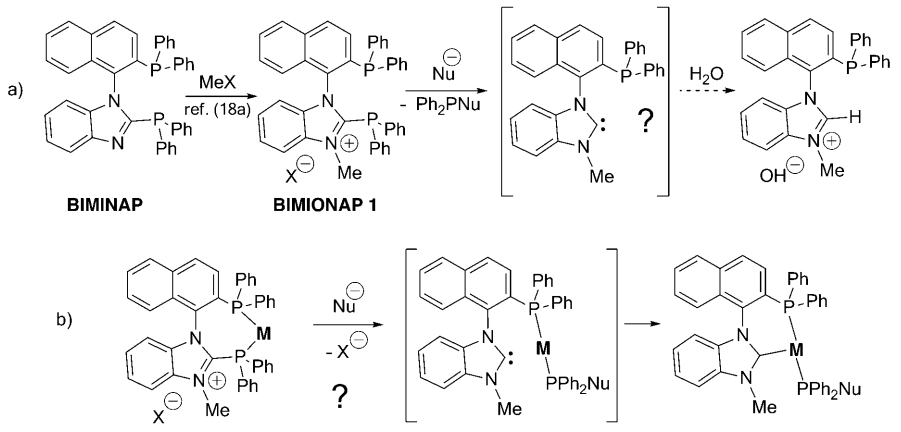

Scheme 2. Characterization of the possibly displaced NHC donor upon addition of an anionic nucleophile to the BIMIONAP ligand **1**: a) intermolecular trapping by hydrolysis of free BIMIONAP; b) intramolecular trapping strategy of the P,P-coordinated BIMIONAP (M = Pd).

NAP, aiming at obtaining the corresponding NHC–phosphine complex (Scheme 2b).[21]

The results are then confronted with theoretical analyses. In particular, the relative weights of the imidazoliophosphine and NHC–phosphenium resonance forms depicted in Scheme 1 are targeted through ELF analysis.

Experimental reactivity of the N_2C-P bond of BIMIONAP: The reactivity of a chloride ion is first envisaged from palladium complexes of BIMIONAP. The case of free BIMIONAP is then addressed and generalized by using the more nucleophilic *n*-butyl anion.

Reactivity of palladium(II) complexes of BIMIONAP with a chloride ion: The BIMIONAP–$PdCl_2$ complex **2** was prepared by addition of a stoichiometric amount of [Pd-$(CH_3CN)_2Cl_2$] to BIMIONAP (**1**) according to the previously described procedure.[18a] Upon addition of tetraethylammonium chloride (TEACl) to an acetonitrile solution of **2** at room temperature, no reaction took place. At 50 °C, however, a slow degradation of **2** was observed. Monitoring the reaction by ^{31}P NMR spectroscopy indicated the complete disappearance of the signals of **2** ($\delta_p = +18.8$, $+24.0$ ppm) after 3 h and the appearance of two new signals at $\delta_p = +23.2$ and $+80.0$ ppm. The latter chemical shift is characteristic of $ClPPh_2$, whereas the former could be consistently attributed to the NHC–phosphine palladium complex **3** (Scheme 3).

Complex **3** was finally isolated in 62% yield from **2** and fully characterized. The essential information is provided by

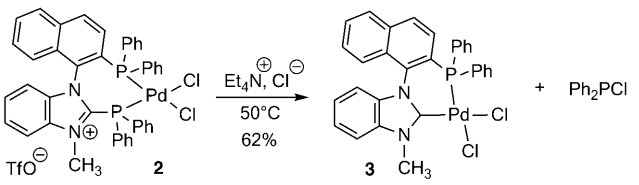

Scheme 3. Formation of the NHC–phosphine palladium complex **3** from the BIMIONAP complex **2**.

the ^{13}C NMR signal at $\delta_C = +170.5$ ppm characteristic of the metal–carbenic NCN carbon atom of **3**, which is strongly deshielded with respect to the corresponding NCN carbon atom of **2** ($\delta_C = +146.1$ ppm, $J_{PC} = 29.4$ Hz). The exact structure of complex **3** was finally confirmed by X-ray diffraction analysis of yellow crystals deposited from a CH_2Cl_2/MeOH/Et_2O mixture at room temperature (Figure 1).[22]

The palladium(II) center adopts a classical square-planar geometry within a pseudo-boat-

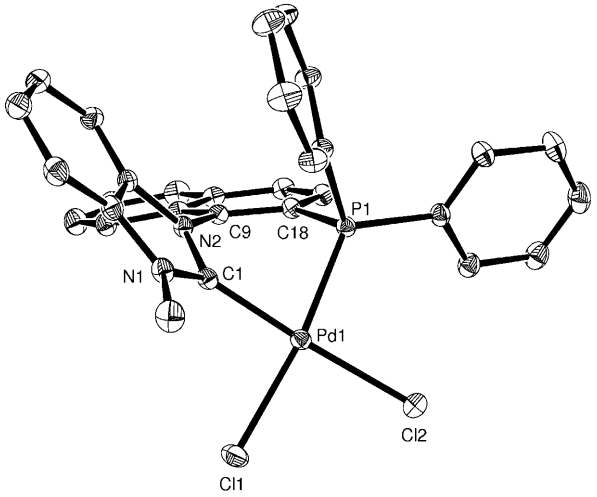

Figure 1. ORTEP view of the X-ray crystal structure of the NHC–phosphine palladium complex **3** (Scheme 3), with thermal ellipsoids drawn at the 30% probability level (for clarity, H atoms are omitted). Selected bond distances [Å] and angles [°]: C1–Pd1: 1.9811(17), P1–Pd1: 2.2405(4), N1–C1: 1.344(2), N2–C1: 1.370(2), Pd1–Cl1: 2.3497(5), Pd1–Cl2: 2.3324(5); C1-Pd1-Cl1: 92.39(5), P1-Pd1-Cl2: 97.011(18), N1-C1-N2: 106.72(15).

shaped six-membered palladacycle. The metal–ligand bond lengths are comparable to those of related NHC–phosphine–$PdCl_2$ complexes.[23] The value of the dihedral angle between the planes of the naphthyl and benzimidazolyl rings (C18-C9-N2-C1: 45.33°) is smaller than in the recently reported NHC–ylide palladium complex homologue (64.10°), for which the ligand backbone is involved in a less strained seven-membered palladacycle.[24]

The formation of the NHC–phosphine–$PdCl_2$ complex **3** from **2** formally results from the nucleophilic displacement of the NHC fragment by the chloride anion at the phosphenium center. This transformation may a priori proceed through three possible mechanisms, depending on the site of initial nucleophilic attack of complex **2**, that is, the Pd, P1, or C1 atom (Scheme 4). Initial attack at Pd could be facili-

tated by the accessible planar geometry and by the vacancy of the 16-electron valence shell of **2**. The palladate intermediate could then undergo migration of one of the chloride ligands to the P1 atom with subsequent or simultaneous cleavage of the P1–C1 bond, as suggested by MacGegor (Scheme 4a-Pd).[25a] Nevertheless, attack at Pd would not be guided by any positive formal charge at the Pd center of **2**: The Cl ligands are covalently bonded to Pd, and the P1 ligands even bring some formal negative charge onto the Pd center as the P→Pd dative bond is equivalent to the α-zwitterionic Lewis structure P^+–Pd^-. The overall partial charge at Pd is indeed calculated to be significantly smaller than the partial charges at P1 (see the section entitled: ELF and AIM-based mesomeric description of BIMIONAP and Scheme 9). Alternatively, direct attack at P1 could thus be driven by the strong P^+ character of this center to give a MacGregor-type pentacoordinate intermediate (Scheme 4a-P).[25a] However, initial attack at P1 remains a priori disfavored because the atom formally satisfies an octet electron count (with no empty low-lying valence orbital) and because of the steric demand at this tetrahedral center. Moreover, both attacks at P1 or Pd lead to N^+/Pd^- γ-zwitterionic palladate species, which are exemplified but still quite energetic.[25b]

In contrast, initial attack at the electrodeficient C1 center (see the section entitled: ELF and AIM-based mesomeric description of BIMIONAP and Scheme 9) instantly reduces the +/− charge separation and can be followed by a classical α-elimination process at a chlorinated sp^3 carbon center. The corresponding likely mechanism is shown in Scheme 4a-C (further argumentation is given in the section entitled: ELF and AIM-based mesomeric description of BIMIONAP).

Whatever the mechanism is, however, cleavage of a P–C bond by a chloride ion selectively bonding to the P atom is rather unusual and is definitively indicative of a dative carbene→phosphenium bond in the amidiniophosphine complex **2**.

Treatment with free chloride ions was then envisaged from the homologous BIMIONAP–Pd(π-allyl) complex. This complex was first targeted by reaction of BIMIONAP (**1**) with a stoichiometric amount of [Pd(π-allyl)Cl]$_2$, but all attempted experimental conditions (solvent, temperature) lead to nonselective decomposition products of BIMIONAP. By following the preceeding observations, this result could be interpreted by the dissociation of free chloride from the PdCl center, which would instantaneously result in the decomposition of free BIMIONAP (see the section entitled: Reactivity of the free BIMIONAP cation with chloride and *n*-butyllithium anions) or of the putative [Pd(allyl)(BIMIONAP)Cl] primary product.

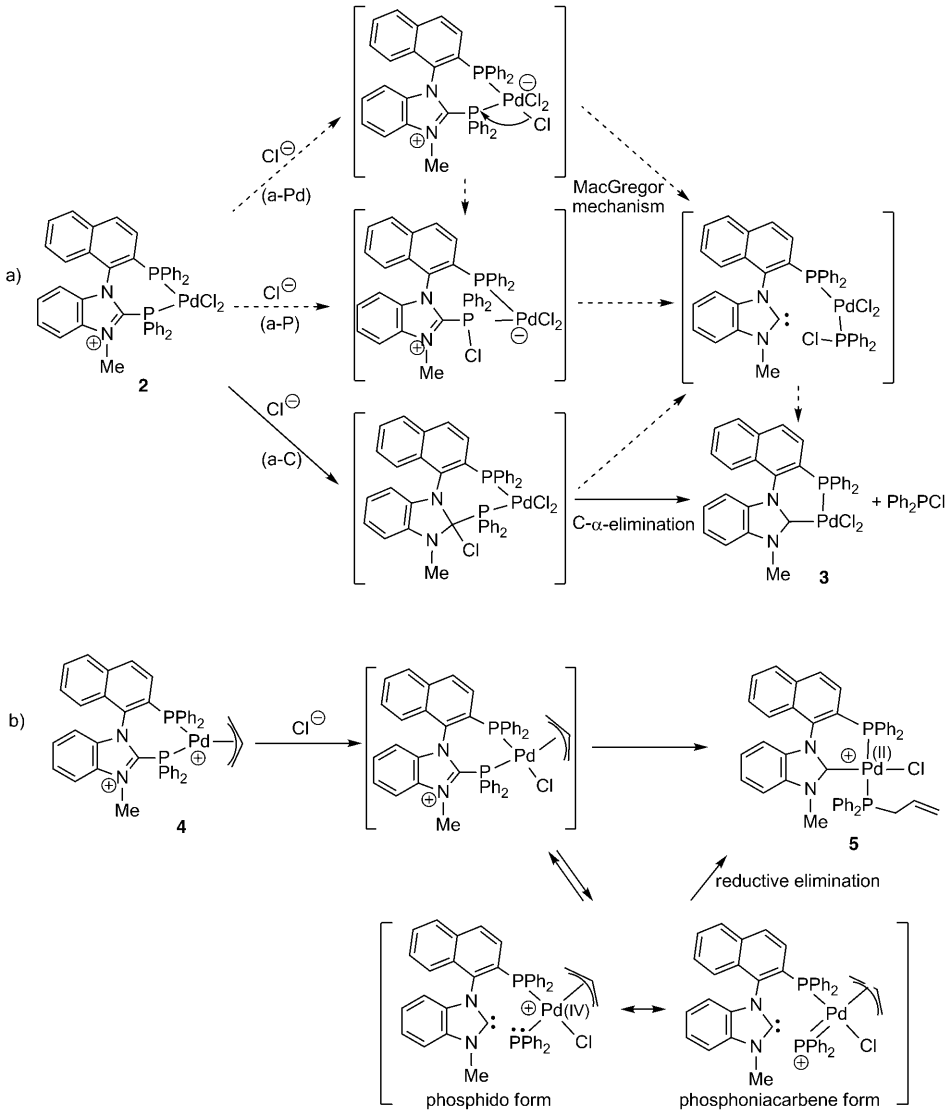

Scheme 4. Possible mechanisms for the formation of NHC–phosphine palladium complexes: a) formation of the $PdCl_2$ complex **3** from the cationic complex **2**. A priori possible mechanisms: a-P) and a-Pd) starting with attack of Cl^- at the P1 or Pd atoms and ending with a MacGregor-type rearrangement, and likely mechanism a-C initiated by attack of Cl^- at the C1 atom resulting in an instant cancellation of the formal charge separation. b) Formation of the $[PdCl(Ph_2Pallyl)]^+$ complex **5** from the dicationic complex **4**; likely mechanism initially driven by the charge deficiency at the Pd center and passing through a formal resonance-stabilized Pd^{IV} intermediate.

A nonchlorinated [Pd(π-allyl)] precursor was thus envisaged. Treatment of **1** with the 'chloride free' [Pd(allyl)-$(MeCN)_2$][TfO] cationic complex[26] in CH_2Cl_2 afforded the targeted complex as a mixture (60:40) of two diastereoisomers **4a**,**b** in 84% yield (Scheme 5). The presence of two diastereoisomers is attributed to a slow 180° rotary flip of the π-allyl ligand and to the restricted rotation of the N_2C-P-Pd-P-Napht unit within the seven-membered metallacycle. The ^{31}P NMR spectroscopic chemical shifts of **4a** and **4b** ($\delta_P = 17.5$, 21.1 ppm, $J_{PP} = 40.8$ Hz; 18.0, 24.1 ppm, $J_{PP} = 41.5$ Hz) are close to those of complex **2** ($\delta_P = 18.8$, 24.0 ppm), whereas the dicationic character of **4** was definitively confirmed by mass spectroscopy (electrospray MS: m/z: 923 $[M^{2+} + OTf^-]^+$). In the ^{13}C NMR spectrum, the two NCN carbon atoms of **4a**,**b** resonate at $\delta_c = +148.5$ (d, $J_{CP} = 15.7$ Hz) and +148.1 ppm (d, $J_{CP} = 18.0$ Hz), respectively.

The dicationic complex **4** (**4a**+**4b**) was then reacted with TEACl in MeCN, and by contrast to complex **2**, the reaction proceeded at room temperature, due to the enhanced electrophilicity of **4**. Monitoring the reaction by ^{31}P NMR spectroscopy indicated the disappearance of **4** and the appearance of two new signals at $\delta_P = +17.76$ (d) and +15.13 ppm (d) with a large P–P coupling constant ($J_{PP} = 457.9$ Hz), along with the signals of the above described complex **3**. After column chromatography, the complexes **3** and **5** were isolated in 29 and 60% yield, respectively. In the ^{13}C NMR spectrum of **5**, a deshielded signal at $\delta_c = 170.5$ ppm (dd, $J_{CP} = 6.8$, 11.5 Hz) is the signature of a Pd-coordinated carbenic carbon atom in the vicinity to two nonequivalent phosphorus atoms, themselves positioned in a *trans* position ($J_{PP} = 457.9$ Hz).

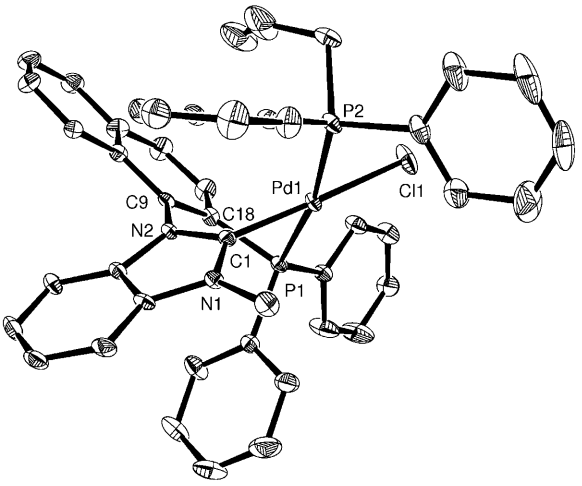

Figure 2. ORTEP view of the X-ray crystal structure of the NHC–phosphine palladium complex **5** with thermal ellipsoids drawn at the 30% probability level (for clarity, triflate anion and H atoms are omitted). Selected bond distances [Å] and angles [°]: C1–Pd1: 1.983(5), P1–Pd1: 2.3183(14), P2–Pd1: 2.3145(15), N1–C1: 1.323(7), N2–C1: 1.356(6), Pd1–Cl1: 2.3144(14); C1-Pd1-Cl1: 176.74(16), P1-Pd1-P2: 169.62(5), N1-C1-N2: 107.8(4).

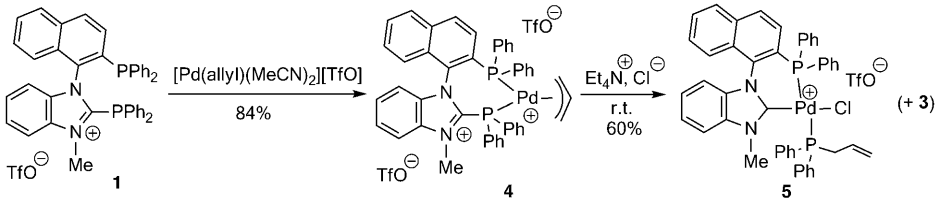

Scheme 5. Synthesis of the cationic P,P- and P,C-chelated palladium complexes **4** and **5**, respectively.

As in the case of **3**, the formation of **5** results from the cleavage of the N_2C–P bond of BIMIONAP. In the present case, however, initial attack at the cationic Pd center, which is likely to be more electronegative than the C1 atom, also instantly reduces the +/− charge separation. The process would now go through a formal phosphide–Pd^{IV} intermediate, stabilized by resonance with a phosphoniacarbene–Pd^{II} form (Scheme 4b). A related complex resulting from oxidative addition of a P–Br bond to a Pd^0 center was recently described by a divalent phosphenium=Pd structure.[2d] In the present case, the Pd^{IV}/Pd^{II} species would then undergo a converse process, namely reductive elimination of the phosphide and allyl ligands producing the allyldiphenylphosphine complex **5**. Beyond mechanistic issues, the two BIMIONAP complexes **2** and **4** behave globally in a similar manner towards the chloride anion, which induces the cleavage of the assumed dative NHC→phosphenium bond to give a transient NHC unit. The latter is immediately trapped by the vicinal palladium center affording the NHC–phosphine-chelated complexes **3** and **5**.

Reactivity of the free BIMIONAP cation with chloride and n-butyllithium anions: By following the procedure used for the BIMIONAP complex **2** (see the section entitled "Reactivity of palladium(II) complexes of BIMIONAP with a chloride ion"), the free BIMIONAP cation **1** was treated with one equivalent of TEACl in MeCN at 50°C. After 3 h, the ^{31}P NMR spectrum indicated the complete disappearance of the signals of **1** ($\delta_P = -18.6$, −16.3 ppm, $J_{PP} = 35.5$ Hz) giving way to a slightly more deshielded signal at $\delta_P = -15.6$ ppm.[27] The ^1H NMR spectrum showed a signal at $\delta_H = 9.4$ ppm in the classical range of iminium CH protons (Scheme 6). The imidazoliophosphine **6** was finally isolated in 66% yield and its structure was confirmed by multinuclear NMR spectroscopy and mass spectrometry technics.

The iminium **6** is the signature of the formation of a transient free NHC, which would be protonated by the MeCN solvent.

The displacement of a NHC moiety from a P atom by such a weak nucleophile as Cl^- is indicative of the NHC→phosphenium dative character of the N_2C–P bond in non-coordinated BIMIONAP.

A similar procedure was conducted at −78 °C with *n*BuLi as a stronger and likely harder nucleophile (instead of Cl^-), and in THF as a nonprotic solvent (instead of MeCN). To trap the expected but elusive free NHC product, the reaction was carried out in the presence of elemental sulfur (S_8), a classical trapping agent of carbenes (Scheme 6). Monitoring the reaction by ^{31}P NMR spectroscopy indicated the immediate disappearance of the starting BIMIONAP (**1**) and the presence of two new signals at $\delta p = +42.7$ and +43.5 ppm. After purification, these two signals were assigned to thio(butyl)diphenylphosphine and thiophosphine-thiourea **7** which was isolated in 71 % yield, respectively.[28]

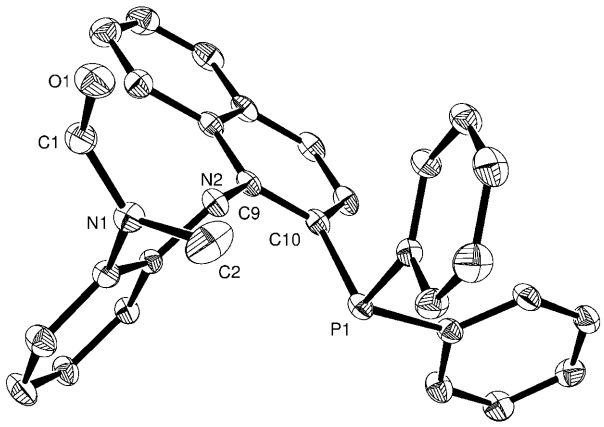

Figure 3. ORTEP view of the X-ray crystal structure of the *o*-phenylenediamine derivative **8** with thermal ellipsoids drawn at the 30 % probability level (for clarity, H atoms are omitted). Selected bond distances [Å] and angles [°]: C1–N1: 1.340(2), C2–N1: 1.455(3), C1–O1: 1.218(2), C10–P1: 1.8371(17); N1-C1-O1: 124.38(18).

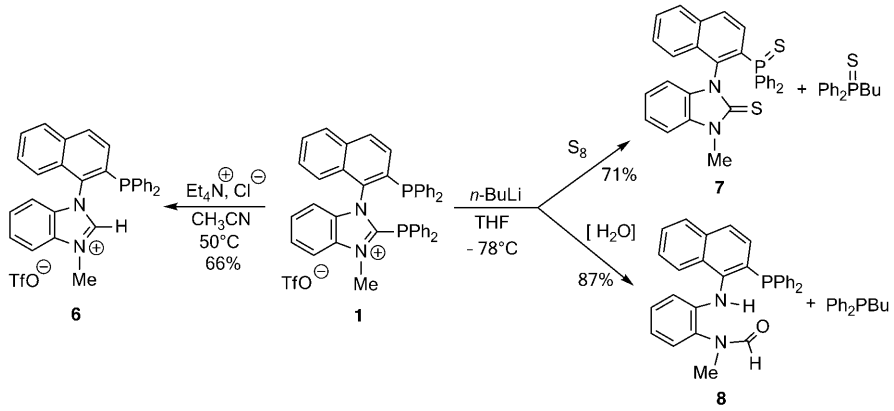

Scheme 6. Reactions of free BIMIONAP with chloride and alkyl anions, followed by treatment with protic sources (MeCN, H_2O) or elemental sulfur (S_8).

The formation of **7** is a signature of the generation of the transient free carbene. Isolation or detection of the latter was finally envisaged.

If the same reaction (BIMIONAP + *n*BuLi in THF) is carried out in the absence of sulfur, the expected butyl(diphenyl)phosphine is produced (^{31}P NMR: $\delta = -16.0$ ppm)[29] along with the phosphine–formamide **8** (^{31}P NMR: $\delta = -16.3$ ppm), which was isolated in 87 % yield and the structure of which was confirmed by an X-ray diffraction analysis (Figure 3).[22] The formation of the *o*-phenylenediamine derivative **8** results from a hydrolytic opening of a benzimidazole ring, which may be explained by the presence of residual water molecules in the starting BIMIONAP (**1**).[30] All attempts to characterize the free NHC in situ by VTP NMR experiments after drying beforehand the hygroscopic BIMIONAP crystals were, however, unsuccessful.

By analogy with the mechanism proposed for the reaction of a Cl^- anion with the P-coordinated BIMIONAP ligand in complex **2** (see the section entitled: Reactivity of palladium(II) complexes of BIMIONAP with a chloride ion, Scheme 4a-C), the mechanism operating in the degradation of free BIMIONAP could also be initiated by nucleophilic attack of Cl^- at the C1 atom, followed by α-elimination of the diaminocarbene and Ph_2PCl (Scheme 7a). Alternatively, and especially for the *n*BuLi nucleophile from which the α-elimination process is less likely, the initial attack could occur at the phosphorus center to give a neutral phosphonium *C*-diamino-ylide intermediate (Scheme 7b). The *C*-diamino-ylide being highly destabilized,[31] it could then undergo dissociation to the neutral phosphine and the neutral diaminocarbene, which would be stabilized by protonation, sulfurization, or hydrolysis (Scheme 7b).

Theoretical analysis of the nature of the N_2C–P bond of BIMIONAP: In a complementary approach, the nature of the N_2C–P bond of BIMIONAP and its reactivity towards nucleophiles were investigated with suitable theoretical tools, in particular, ELF[32] and atoms in molecules (AIM) analyses.[33]

Dative nature of the N_2C–P bond of BIMIONAP in the gas phase: The preferred dissociation mode of the N_2C–P bond for a model of BIMIONAP (**1**) has been calculated in the gas phase at the B3PW91/6-31G** level of theory (Scheme 8). The heterolytic mode ($D_{hetero} = 76.9$ kcal mol^{-1}, ZPE-corrected value) is found to be favored by about 15 kcal mol^{-1} over the homolytic mode ($D_{homo} = 91.8$ kcal

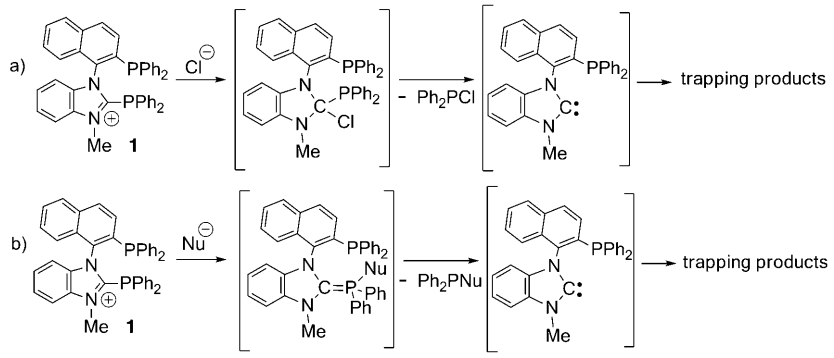

Scheme 7. Possible mechanisms for the nucleophilic degradation of free BIMIONAP: a) initial attack at the C1 center by a Cl^- ion, followed by α-elimination of Ph_2PCl (see analogy with the proposed mechanism for the Cl_2Pd–P-coordinated BIMIONAP in complex **2** (Scheme 4a-C); b) intitial attack at the P1 atom to give an unstable phosphonium *C*-diamino-ylide. In both mechanisms, the released NHC would be trapped in situ by protonation, hydrolysis, or sulfurization (see Scheme 6).

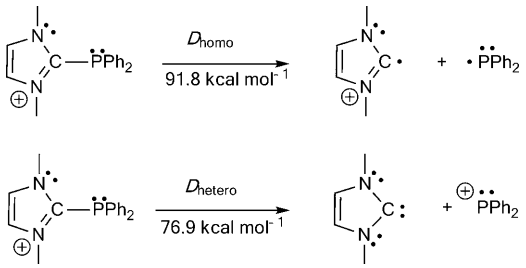

Scheme 8. Homolytic (top) and heterolytic (bottom) dissociation schemes and corresponding energies (B3PW91/6-31G** level of calculation) of a model of BIMIONAP (**1**).

mol^{-1}, ZPE-corrected value). This result is in complete accordance with the experimental results.

ELF- and AIM-based mesomeric description of BIMIONAP: From a general standpoint, the ELF partition of the molecular space provides basins that correspond to the cores, lone or shared-pairs of the Lewis model.[32] Their mean populations and (co)variances can be interpreted in terms of weighted combinations of mesomeric structures.[34] The method is here applied to the N_2C–P bond in both the free cation **1** and the BIMIONAP palladium dichloride complex **2** (Scheme 9).

AIM atomic charges and scaled populations[35] of the ELF valence basins of the carbene phosphenium moieties of **1** and **2** are very similar (Scheme 9). The same Lewis forms can, therefore, be invoked for their mesomeric description. In the ELF-based description of Scheme 10b, the C→P^+ symbol is not strictly equivalent to the C^+–P Lewis symbol of Scheme 10a because it has the additional meaning that the N_2C–P bond is energetically labile (an indirect criterion for a donor–acceptor interaction) and dissociates in a heterolytic manner. This description is in agreement with literature data on related compounds[17,18] that concluded to "dative C→P bonds" according to the definition of Mulliken[1a–b] and Haaland,[1c] that is, polar bonds with an energetically more favorable heterolytic cleavage. According to the mesomeric description of Scheme 10b, BIMIONAP is thus expected to retain significant σ-donating properties as the lone pair of P1 is not involved in the electron delocalization. Moreover, P1 and P2 atoms are hardly distinguishable from the AIM charges and ELF populations of the monosynaptic *V*(P) basin corresponding to their lone pair. Only the shift in population of the P–C disynaptic basins (*V*(P1,C1): 2.62; *V*(P2,C10): 2.31) allows us to distinguish between the P2−C2 and P1−C1 bonds (Scheme 9). It is noteworthy that the excess of electrons in the P1−C1 bond cannot be attributed to a P1=C1

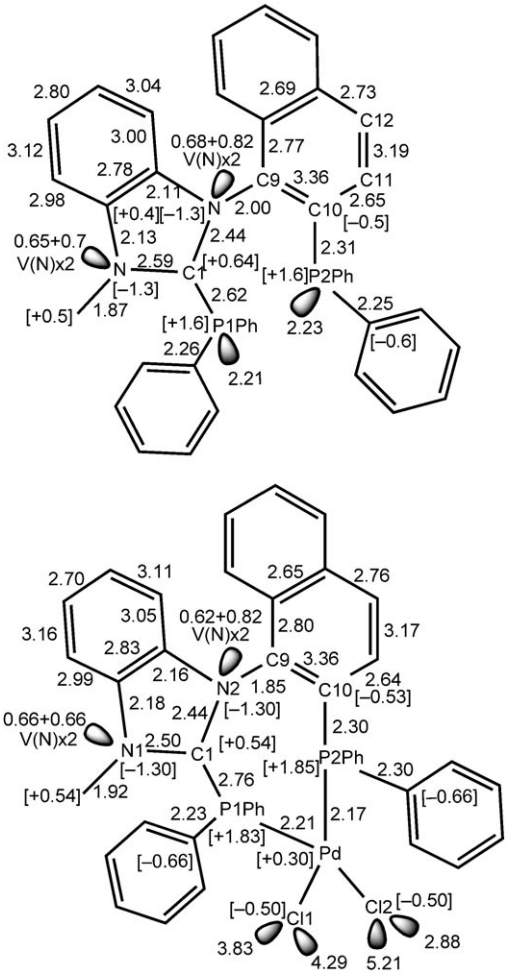

Scheme 9. Scaled populations of selected ELF valence basins of free BIMIONAP (**1**) (top; B3PW91/6-31G** level of calculation) and BIMIONAP–Pd complex **2** (bottom; B3PW91/6-31G**/DGDZVP(Pd) level of calculation). AIM charges are given in square brackets.

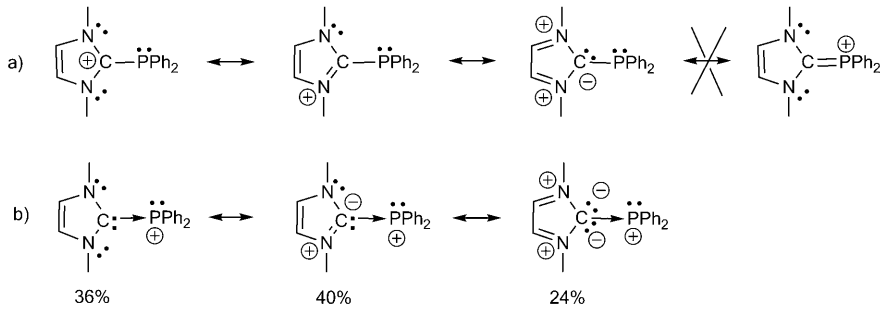

Scheme 10. Mesomeric descriptions of the imidazoliophosphine unit of BIMIONAP (the remainder of the structure is omitted for clarity). a) Lewis topological mesomerism. b) Topological-energetical mesomerism by using a dative bond symbol reflecting the lability and the heterolytic dissociation preference of the N_2C–P bond: the weights are determined from the ELF valence basins populations and covariances (Scheme 9).

double character because the bond length is typical of a pure single bond (1.847 Å vs. an even shorter length of 1.808 Å in the neutral nonmethylated BIMINAP precursor depicted in Scheme 11).[18a]

ELF- and AIM-based electrophilic Fukui indices of BIMIONAP: Insights into the mechanism of the observed N_2C–P bond cleavage (see the section entitled: Experimental reactivity of the N_2C–P bond of BIMIONAP and Scheme 4) have been gained within the framewok of a "pre-reacting" approach, thus focusing on the early stage of the process. The electrophilicity of BIMIONAP was thus investigated by using two complementary analytical tools,[36] namely, the molecular electrostatic potential (MESP) and the Fukui function. The former index is suitable for the description of hard–hard or charge-controlled interactions, whereas the latter will allow for probing soft sites of the molecules that are involved in orbital-controlled interactions with electrophiles, nucleophiles, or radicals. The Fukui function was introduced by Parr and Yang as a generalization of Fukui's frontier molecular orbitals (FMO) concept as the response of the electron density of the molecular system to a change in the global number of electrons.[37] It can be expressed as the derivative of the electron density $\rho(r)$ with respect to the number of electrons N, calculated at constant external potential $v(r)$. Because of the discontinuity induced by the discrete intrinsic nature of N, left and right derivatives have to be considered. The local Fukui functions $f^+(r)=(\partial\rho/\partial N)^+_v$ and $f^-(r)=(\partial\rho/\partial N)^-_v$ are the respective response for adding or removing electrons from the system and allowing, therefore, for an investigation of nucleophilic and electrophilic attacks, respectively (radical attack is assumed to be correlated with $f^0(r)=1/2[f^+(r)+f^-(r)]$). The finite difference approach ($\Delta N=\pm1$) yielding the following expressions [Eq. (1) and (2)] of the local Fukui function $f(r)$ has been extensively used for the estimation of atomic Fukui indices f(A) from atomic charges:[38]

$$f^+(r)\approx\rho_{N+1}(r)-\rho_N(r)\rightarrow f^+(\mathrm{A})=Q_N(\mathrm{A})-Q_{N+1}(\mathrm{A}) \quad (1)$$

$$f^-(r)\approx\rho_N(r)-\rho_{N-1}(r)\rightarrow f^-(\mathrm{A})=Q_{N-1}(\mathrm{A})-Q_N(\mathrm{A}) \quad (2)$$

in which $Q_{N+\varepsilon}$(A) denotes the atomic charge (Mulliken, NPA, AIM) of the atom A.

Recently, alternative condensation schemes of frontier molecular orbital Fukui functions within an AIM[39] or ELF[40] topological partition have been disclosed [Eq. (3)]:

$$f^\alpha_X=\int_X|\phi^F_{KS}(r)|^2dr \quad (3)$$

Equation (3) expresses the contribution of the FMO F to the atomic AIM basin or to the core or valence ELF basin X ($\alpha=+$: F=LUMO; $\alpha=-$: F=HOMO). These indices are more attractive than the above atomic indices because they are confined in the 0–1 range and they sum to one: $0\le f^\alpha_X\le1$ and $\Sigma_x f^\alpha_X=1$. The larger the value of f^α_X, the more reactive the corresponding site X. The dual reactivity descriptor $\Delta f=f^+(r)-f^-(r)$ can also be used for the simultaneous detection of nucleophilic or electrophilic behavior of a given site and is particularly useful for ambiphilic reactants.[41]

Fukui functions f^+, characterizing the reactivity towards nucleophilic attack, condensed on ELF or AIM basins, were calculated for BIMIONAP and its neutral parent BIMINAP[18a] at the B3PW91/6-31G** level (Scheme 11, Table 1). The largest f^+_{ELF} value (0.16) is thus obtained for the P1–C1 bond of BIMIONAP, in agreement with the experimental observations that this bond is the most sensitive to nucleophilic attack (see the section entitled: Reactivity of the free BIMIONAP cation with chloride and *n*-butyllithium anions). The largest f^+_{AIM} value calculated for the C1 atom (0.24) points to the latter as the most reactive site towards sufficiently soft nucleophiles. In contrast, the lower f^+_{AIM} value calculated for the P1 atom (0.06) suggests that the latter is more prone to react with hard nucleophiles. The free chloride Cl^- is bigger and thus softer than the carbanionic atom of the nBu$^-$ anion. Moreover, the latter is made

Table 1. Selected values of Fukui functions f^+ condensed on ELF or AIM basins for BIMINAP and BIMIONAP. See atom labelling in Schemes 9 and 11.

BIMINAP			BIMIONAP (**1**)		
ELF basin	f^+_{ELF}	Δf_{ELF}	ELF basin	f^+_{ELF}	Δf_{ELF}
***V*(C1, P1)**	**0.00**	**−0.01**	**V(C1,P1)**	**0.16**	**0.16**
V(C9, C10)	0.09	0.04	V(C1,N1)	0.05	0.05
V(C10, C11)	0.07	0.06	V(P2)	0.05	0.04
AIM basin	f^+_{AIM}	Δf_{AIM}	AIM basin	f^+_{AIM}	Δf_{AIM}
C9	0.16	0.10	**P1**	**0.06**	**0.05**
C11	0.13	0.11	**C1**	**0.24**	**0.24**
P1	0.00	0.00	N2	0.10	0.10
P2	0.02	−0.27	P2	0.01	−0.34

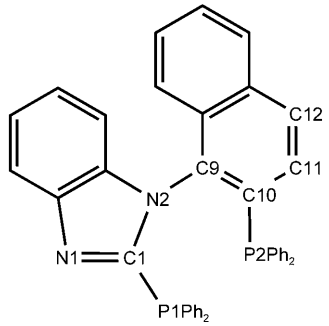

Scheme 11. Atom labelling for Fukui indices for BIMINAP. Values of ELF basin populations, AIM charges and Fukui indices are given in Table 1. The same labeling is adopted for the Pd complex in Table 2.

Table 2. Selected values of Fukui functions f^+ condensed on ELF or AIM basins for the $PdCl_2$ complexes of BIMINAP and BIMIONAP complex **2**. See atom labelling in Scheme 11.

[Pd(BIMINAP)Cl_2]			[Pd(BIMIONAP)Cl_2] (**2**)		
ELF basin	f^+_{ELF}	Δf_{ELF}	ELF basin	f^+_{ELF}	Δf_{ELF}
***C*(Pd)**	**0.12**	**0.10**	***C*(Pd)**	**0.11**	**0.10**
***V*(P1,C1)**	**0.03**	**0.03**	**V(P1,C1)**	**0.15**	**0.15**
V(P2,C10)	0.04	0.04	V(P2,C10)	0.03	0.03
V(C9,C10)	0.06	0.06	V(C1,N)	0.03	0.03
V(C10,C11)	0.04	0.04	V(C9,C10)	0.03	0.02
V(C11,C12)	0.04	0.04	V(Cl)	0.03	−0.18
V(Pd,P1)	0.02	0.01	V(Pd,P2)	0.02	0.01
V(Pd,P2)	0.02	0.01	V(Pd,P1)	0.01	0.01
AIM basin	f^+_{AIM}	Δf_{AIM}	AIM basin	f^+_{AIM}	Δf_{AIM}
Pd	**0.12**	**0.10**	**Pd**	**0.12**	**0.10**
C1	**0.03**	**0.03**	**C1**	**0.20**	**0.20**
C9	0.12	0.12	N1	0.09	0.09
C10	0.07	0.07	C9	0.04	0.03
C12	0.09	0.09	C10	0.05	0.04
P1	0.03	0.02	P1	0.02	0.02
P2	0.04	0.02	P2	0.04	0.03

even harder through its interaction with the very hard Li^+ cation in *n*BuLi. According to Pearson indeed the hardness (η) of anionic atoms is approximately equal to the hardness of the corresponding radicals[42] and $\eta(Cl) = 4.7\,eV < \eta(C) = 5.0\,eV$. The soft chloride ion would thus react at the C1 atom, in agreement with the mechanism proposed in Scheme 7a. In contrast, the harder carbanionic center of *n*BuLi could react in a charge-controlled manner at the harder P1 center of the C1–P1 bond. The P1 atom being 2.5 times more positively charged than the C1 atom ($Q_{AIM}(P1) = 1.6 \gg Q_{AIM}(C1) = 0.64$, Scheme 9), the attack of the hard *n*BuLi nucleophile is charge-controlled at the P1 center, in agreement with the mechanism proposed in Scheme 7b.

In the neutral parent BIMINAP, both the P–C bonds are equivalent and are predicted to be insensitive to nucleophilic attack because of their low computed f^+ values (Table 1), in agreement with experimental observations.[43]

In the [Pd(BIMIONAP)Cl_2] complex **2**, the values of f^+_{ELF} are the largest for the N_2C–P bond (0.15) and the Pd center (0.11), and almost vanish at the P–Pd bonds (Table 2). The P1–Pd bond is thus predicted to be cleavage-resistant in the early stage of the process, as proposed in Scheme 4a-C. The largest f^+_{AIM} value occurs at the C1 atom (0.20; it is almost two times smaller at the Pd atom: 0.12). As in the case of free BIMIONAP (Scheme 7a), the initial attack of **2** by the soft Cl^- anion is predicted to occur at the C1 center. All these results finally support the mechanism proposed in Scheme 4a-C. For comparison, in the neutral [Pd(BIMINAP)Cl_2] complex, the Pd center exhibits f^+_{AIM} and f^+_{ELF} values similar to those of the BIMIONAP parent **2**, but the reactivity of the C1–P1 bond is found to vanish: f^+_{ELF} (V(P1,C1)) = 0.03 ($\ll$0.15 for **2**), f^+_{AIM} (C1) = 0.03 ($\ll$0.20 for **2**).

Frontier molecular orbitals of BIMIONAP: The near-frontier molecular orbitals calculated for the experimental geometry of BIMIONAP (**1**) and BIMINAP at the B3PW91/6-31G** level are displayed in Figure 4.

The LUMO of BIMIONAP (**1**) results from the overlap of the π*(NHC) antibonding orbital of the benzimidazolium moiety with the p_π HOMO of the diphenylphosphenium moiety. It is much lower in energy than the LUMO+2 of the parent BIMINAP resulting from the same type of fragment orbital overlap. This is in agreement with the high electrophilicity of the P1–C1 bond of **1** and further suggests that this ligand should possess sizeable π-accepting properties.

The HOMO of BIMIONAP (occupied by the lone pair of P2) and the HOMO-1 and HOMO-3 (exhibiting a sizeable weight on P1) are much deeper in energy than the corresponding HOMO and HOMO-1 of the parent BIMINAP. The BIMIONAP ligand is, therefore, expected to be much less σ-donating than the BIMINAP ligand.

The LUMOs of the complexes [Pd(BIMIONAP)Cl_2] (**2**) and [Pd(BIMINAP)Cl_2] are displayed in Figure 5 (for the XRD geometry and at the B3PW91/6-31G**/DGDZVP level of calculation). The LUMO of **2** is much lower in energy and thus much more reactive than that of the neutral BIMINAP complex, in agreement with both expectation and experimental observations. The LUMO of **2** is comparable in shape and location to the LUMO of the free ligand **1**. This suggests that the P1–C1 bond of **2** is the most sensitive to attacks by sufficiently soft nucleophiles, in agreement with the mechanism proposed in Scheme 4a-C, and with the predictions of the ELF-condensed Fukui indices (see the section entitled: ELF- and AIM-based electrophilic Fukui indices of BIMIONAP and Table 2).

Molecular electrostatic potential of BIMIONAP: The molecular electrostatic potential (MESP) has been extensively used for probing molecular structure and reactivities.[44] It corresponds to the potential generated by the molecular charge distribution as experienced by a positive point charge [see Eq. (4)]:

$$V(r) = \sum_A \frac{Z_A}{|r - R_A|} - \int \frac{\rho(r')}{|r - r'|} d^3r' \qquad (4)$$

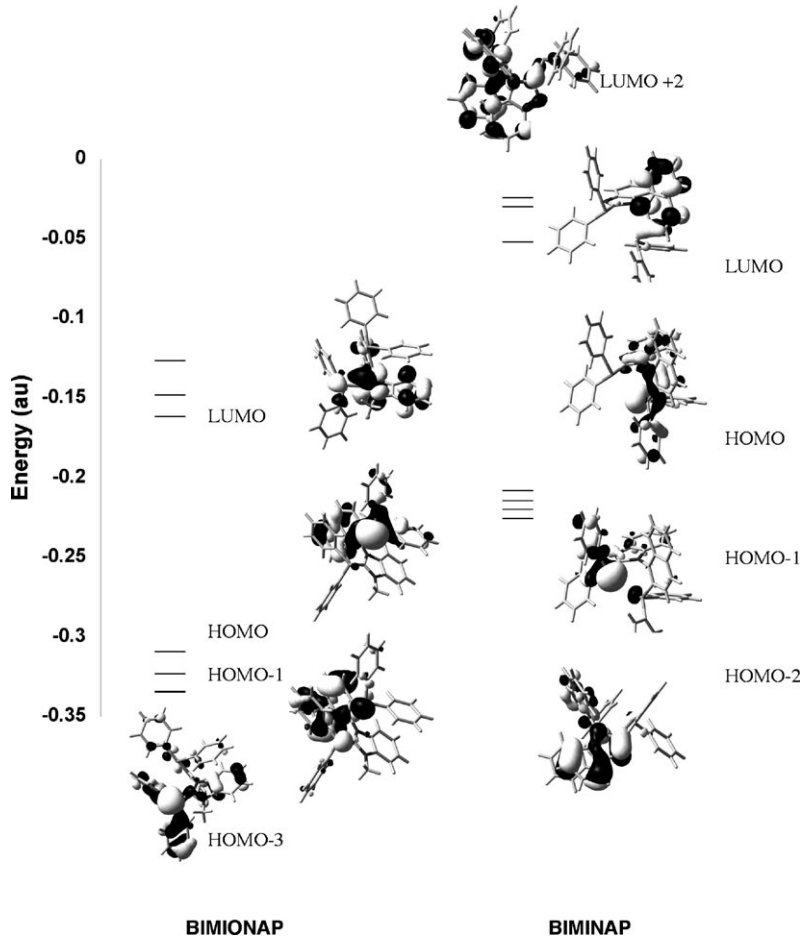

Figure 4. Near-frontier orbitals of BIMIONAP (**1**) and BIMINAP (B3PW91/6-31G** level of calculation).

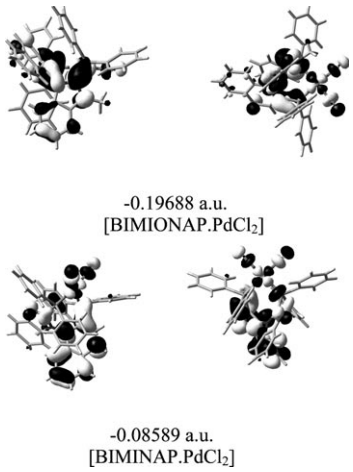

Figure 5. LUMOs of palladium complexes of BIMIONAP complex **2** and BIMINAP (B3PW91/6-31G**/DGDZVP level of calculation).

in which Z_A denotes the nuclear charges, R_A the position of the nuclei, and $\rho(r)$ the electron density.

The MESP minima indicate the concentration sites of electron density and the most favorable sites of electrophilic attack.[45] For nucleophilic attacks, since the maxima of MESP are exclusively located at nuclear positions, it is convenient to use MESP textured on isodensity surfaces for exploring the regions of positive MESP and finding the most electrodeficient sites. Such surfaces have been obtained for BIMINAP, BIMIONAP, and their $PdCl_2$ complexes (Figure 6).

These plots indicate that the most positive MESP region is located near the P1–C1 bond of both the free BIMIONAP (**1**) and its palladium complex **2**. This result is in agreement with the electrophilic reactivity of the P1–C1 bond towards the Cl^- and nBu$^-$ anions (see the section entitled: Experimental reactivity of the N_2C–P bond of BIMIONAP). Finally, both the orbitals and the charges tend to control nucleophilic attack at the C1–P1 bond. In the corresponding regions of the parent free BIMINAP or [Pd(BIMINAP)Cl_2] complex, the MESP is much less positive, in agreement with the observed insensitivity of the P1–C1 bond towards nucleophilic attack.

All the computed reactivity indices are, therefore, consistent with the mechanisms of Schemes 4a, 7a, and 7b reflecting that the P1–C1 bond of free or Cl_2Pd–P-coordinated BIMIONAP is the most sensitive site to nucleophilic attack. These indications could serve as guides for a complete mechanistic study (of much higher computational cost) through the exploration of the potential energy surface versus suitable reaction coordinates.

Conclusion

Addition of anionic nucleophiles (Cl^-, nBu$^-$) to free BIMIONAP (**1**) and BIMIONAP-containing palladium complexes (**2**, **4**) results in selective cleavage of the N_2C–P bond, from which the released NHC fragment can be trapped by protonation, hydrolysis, sulfurization, or coordination to Pd^{II} centers. The displacement of a highly reactive NHC fragment by a so called "weak" chloride nucleophile and the unusual transformation scheme C–P + Cl^- → C: + Cl–P are convincing signatures of a donor–acceptor covalent interaction in amidiniophosphines, that are, therefore, better

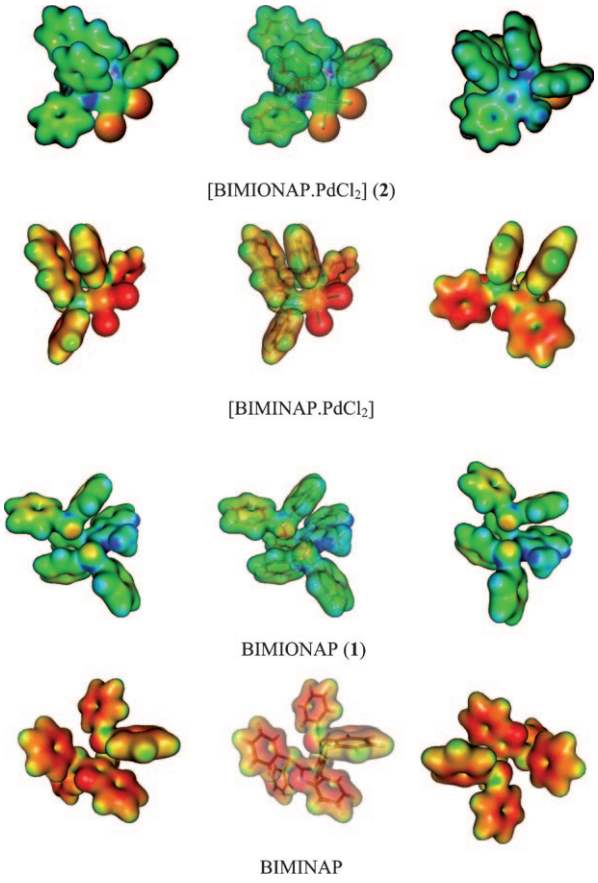

Figure 6. MESP visualization of BIMINAP and BIMIONAP ligands and complexes. Isodensity surfaces (0.02 a.u.) colorcoded with the MESP. Color scale: red: MESP < 0.0; yellow: MESP = 0.1; green: MESP = 0.15; light-blue: MESP = 0.215; dark-blue: MESP > 0.26.

described as NHC→phosphenium adducts, as a priori suggested before by several authors.[17,18] This experimental evidence of a dative bonding is theoretically supported by the comparison of the homolytic and heterolytic DFT-calculated modes of dissociation in the gas phase and by ELF and AIM analysis. Mechanistic issues on the observed electrophilic reactivity of BIMIONAP are also gained from analyses of the molecular orbitals, Fukui indices condensed on ELF- and AIM basins, and MESP. Beyond the fundamental information gained on the nature of NHC→phosphenium interactions, the disclosed results pave the way for numerous developments, for example, by using other weak nucleophiles and the possibly neutral nucleophiles. Finally, finding applications of the disclosed reactivity on the enantiomerically resolved atropochiral BIMIONAP ligand is a natural challenge in the field of stereoselective synthesis and asymmetric catalysis.

Experimental Section

General remarks: THF and diethyl ether were dried and distilled over sodium/benzophenone, pentane, dichloromethane, and acetonitrile over CaH_2. All other reagents were used as commercially available. All reactions were carried out under an argon atmosphere, by using schlenk and vacuum line techniques. Column chromatography was carried out on silica gel (60 Å, C.C 70–200 μm). The following analytical instruments were used. ^1H, ^{13}C, and ^{31}P NMR spectroscopy: Bruker ARX 250, DPX 300, and AV 500. NMR chemical shifts δ are in ppm, with positive values to high frequency relative to the tetramethylsilane reference for ^1H and ^{13}C and to H_3PO_4 for ^{31}P.

Compound 3: A mixture of tetraethylammonium chloride (0.109 g, 0.66 mmol) and [Pd(BIMIONAP)Cl_2] (**2**) (0.418 g, 0.44 mmol) was dissolved in CH_3CN (20 mL) and stirred at 50 °C for 3 h. After evaporation of the solvent, the solid residue was purified by flash chromatography on silica gel (CH_2Cl_2/acetone) to afford a yellow solid (yield: 0.17 g, 62 %). Recrystallisation at room temperature from a CH_2Cl_2/MeOH/Et_2O mixture gave complex **3** as yellow crystals (dec. p. 250 °C); $^{31}P\{^1H\}$ NMR ($CDCl_3$, 25 °C): $\delta = +23.16$ ppm; ^1H NMR ($CDCl_3$, 25 °C): $\delta = 8.08$ (d, $J_{HH} = 8.4$ Hz, 1H; H_{ar}), 8.03 (d, $J_{HH} = 8.2$ Hz, 1H; H_{ar}), 7.75 (pseudot, $J_{HH} = 7.2$, 7.6 Hz, 1H; H_{ar}), 7.67 (d, $J_{HH} = 8.5$ Hz, 1H; H_{ar}), 7.62–7.56 (m, 5H; H_{ar}), 7.53–7.50 (m, 2H; H_{ar}), 7.28–7.24 (m, 4H; H_{ar}), 7.17–7.12 (m, 3H; H_{ar}), 7.04 (pseudot, $J_{HH} = 8.7$, $J_{HP} = 9.5$ Hz, 1H; H_{ar}), 6.74 (d, $J_{HH} = 8.2$ Hz, 1H; H_{ar}), 4.36 ppm (s, 3H; CH_3N); $^{13}C\{^1H\}$ NMR ($CDCl_3$, 25 °C): $\delta = 170.5$ (s, NCN), 138.9 (d, $J_{CP} = 8.6$ Hz; C_{ar}), 136.9 (s, C_{ar}), 136.0 (d, $J_{CP} = 1.9$ Hz; C_{ar}), 135.6 (d, $J_{CP} = 10.5$ Hz; CH_{ar}), 133.5 (s, C_{ar}), 132.5 (d, $J_{CP} = 3.0$ Hz; CH_{ar}), 131.7 (d, $J_{CP} = 2.4$ Hz; CH_{ar}), 129.8 (d, $J_{CP} = 8.6$ Hz; CH_{ar}), 129.2 (s, CH_{ar}), 128.9 (s, CH_{ar}), 128.6 (d, $J_{CP} = 12.0$ Hz; CH_{ar}), 128.3 (brs, CH_{ar}), 128.2 (s, CH_{ar}), 127.2 (d, $J_{CP} = 6.4$ Hz; C_{ar}), 126.9 (d, $J_{CP} = 57.9$ Hz; C_{ar}), 126.5 (d, $J_{CP} = 5.5$ Hz; CH_{ar}), 124.7 (s, CH_{ar}), 124.3 (s, CH_{ar}), 124.1 (s, CH_{ar}), 122.4 (d, $J_{CP} = 55.3$ Hz; C_{ar}), 121.6 (d, $J_{CP} = 54.3$ Hz; C_{ar}), 112.7 (s, CH_{ar}), 110.9 (s, CH_{ar}), 35.9 ppm (s, CH_3N); MS (FAB$^+$): m/z: 583 $[M-Cl]^+$; HRMS (ES$^+$): m/z: calcd for $C_{32}H_{26}ClN_3PPd$: 624.0596; found: 624.0632 $[M-Cl+CH_3CN]^+$.

Compound 4: A mixture of complex bis(acetonitrile)-η^3-allylpalladium triflate (0.106 g, 0.28 mmol) and BIMIONAP (**1**) (0.22 g, 0.28 mmol) was dissolved in CH_2Cl_2 (10 mL) and stirred at room temperature for 2 h. After filtration and evaporation of the solvent, the residue was washed with Et_2O (3×10 mL) to afford a yellow solid as a mixture (60:40) of two diastereoisomers **4a**,**b**. Yield: 0.255 g, 84 %; major isomer = A, minor isomer = B: $^{31}P\{^1H\}$ NMR (CD_3CN, 25 °C): $\delta = +24.09$ (d, $J_{PP} = 41.5$ Hz; P^B), +21.07 (d, $J_{PP} = 40.8$ Hz; P^A), +18.04 (d, $J_{PP} = 41.5$ Hz; P^B), +17.49 ppm (d, $J_{PP} = 40.8$; P^A); ^1H NMR (CD_3CN, 25 °C): $\delta = 8.26$ (dd, $J_{HH} = 7.6$, $J_{HP} = 13.6$ Hz, 1.5H; H_{ar}), 8.18 (dd, $J_{HH} = 7.3$, $J_{HP} = 13.5$ Hz, 2.2H; H_{ar}), 7.93–7.30 (m, 35H; H_{ar}), 7.26–7.10 (m, 6H; H_{ar}), 7.06–7.00 (m, 3.4H; H_{ar}), 6.93–6.89 (m, 1.7H; H_{ar}), 6.75–6.71 (m, 3.7H; H_{ar}), 6.63 (d, $J_{HH} = 8.4$ Hz, 1H; H_{ar}), 6.31–6.22 (m, 1.8H; CH_{allyl}), 5.29–5.25 (m, 1.8H; CH_{2allyl}), 4.56 (pseudot, $J_{HH} = J_{HP} = 5.8$ Hz, 1H; CH_{2allyl}), 4.46 (dd, $J_{HH} = 10.2$, $J_{HP} = 13.9$ Hz, 0.9H; CH_{2Allyl}), 4.39 (dd, $J_{HH} = 11.3$, $J_{HP} = 11.8$ Hz, 0.7H; CH_{2allyl}), 4.27 (pseudot, $J_{HH} = J_{HP} = 5.1$ Hz, 0.7H; CH_{2allyl}), 4.01 (pseudot, $J_{HH} = J_{HP} = 11.8$ Hz, 0.7H; CH_{2allyl}), 3.68 (s, 3H; CH_3N), 3.65 (s, 2.5H; CH_3N), 3.46 ppm (pseudot, $J_{HH} = J_{HP} = 11.4$ Hz, 0.8H; CH_{2allyl}); $^{13}C\{^1H\}$ NMR (CD_3CN, 25 °C): $\delta = 148.5$ (d, $J_{CP} = 15.7$ Hz; C_{ar}), 148.1 (d, $J_{CP} = 18.0$ Hz; C_{ar}), 135.3 (s, C_{ar}), 135.2 (s, C_{ar}), 135.0 (d, $J_{CP} = 16.3$ Hz; CH_{ar}), 134.9 (d, $J_{CP} = 12.6$ Hz; CH_{ar}), 134.3–133.9 (m, C_{ar}; CH_{ar}), 133.5 (d, $J_{CP} = 13.5$; CH_{ar}), 133.3 (C_{ar}), 133.2 (C_{ar}), 132.9 (d, $J_{CP} = 2.3$ Hz; CH_{ar}), 132.5–132.2 (m, C_{ar}; CH_{ar}), 131.6 (d, $J_{CP} = 6.7$ Hz; C_{ar}), 131.2 (d, $J_{CP} = 6.5$ Hz; C_{ar}), 130.6 (d, $J_{CP} = 11.3$ Hz; CH_{ar}), 130.5 (d, $J_{CP} = 12.6$ Hz; CH_{ar}), 129.7 (d, $J_{CP} = 11.3$ Hz; CH_{ar}), 129.5–129.0 (m; C_{ar}, CH_{ar}), 128.8 (d, $J_{CP} = 12.6$ Hz; CH_{ar}), 128.6–128.5 (m; CH_{ar}), 127.7–127.4 (m; C_{ar}, CH_{ar}), 125.8 (d, $J_{CP} = 47.8$ Hz; C_{ar}), 125.5 (t, $J_{CP} = 6.3$ Hz; CH_{allyl}), 125.1 (t, $J_{CP} = 6.3$ Hz; CH_{allyl}), 124.4 (d, $J_{CP} = 43.0$ Hz; C_{ar}), 123.7–123.2 (m; C_{ar}, CH_{ar}), 122.0 (d, $J_{CP} = 47.8$ Hz, C_{ar}), 121.1 (q, $J_{CF} = 320.0$ Hz; $CF_3SO_3^-$), 115.1 (s, CH_{ar}), 115.0 (s, CH_{ar}), 113.4 (s, CH_{ar}), 113.3 (s, CH_{ar}), 84.9 (d, $J_{CP} = 25.0$ Hz; CH_{2allyl}), 80.7 (d, $J_{CP} = 24.4$ Hz; CH_{2allyl}), 79.0 (d, $J_{CP} = 30.0$ Hz; CH_{2allyl}), 75.8 (d, $J_{CP} = 25.0$ Hz; CH_{2allyl}), 36.7 (s, CH_3N), 36.4 ppm (s, CH_3N); MS (FAB): m/z: 923 $[M^2+OTf^-]^+$; HRMS (ES$^+$): m/z: calcd for $C_{46}H_{38}N_2P_2PdF_3SO_3$: 923.1065; found: 923.1052.

Compound 5: A mixture of tetraethylammonium chloride (0.058 g, 0.35 mmol) and [Pd$^+$(allyl)(BIMIONAP)(OTf^-)] (**4**) (0.310 g, 0.29 mmol) was dissolved in CH_3CN (10 mL) and stirred at room temperature for

3 h. After evaporation of the solvent, the solid residue was purified by flash chromatography on silica gel (CH_2Cl_2/acetone) to afford the carbenic complex **3** (yield: 0.052 g, 29%) and the carbenic complex **5** (0.170 g, 60%), respectively, as yellow solids. Recrystalisation of complex **5** at −20°C from a CH_2Cl_2/pentane mixture gave yellow crystals. M.p. 169–172°C; $^{31}P\{^1H\}$ NMR ($CDCl_3$, 25°C): $\delta = +17.76$ (d, $J_{PP} = 457.9$ Hz), +15.13 ppm (d, $J_{PP} = 457.9$ Hz); ^1H NMR ($CDCl_3$, 25°C): $\delta = 8.25$–8.21 (m, 2H; H_{ar}), 7.85 (t, $J_{HH} = 7.5$ Hz, 1H; H_{ar}), 7.74–7.41 (m, 12H; H_{ar}), 7.30–7.09 (m, 12H; H_{ar}), 7.03 (t, $J_{HH} = 7.2$ Hz, 2H; H_{ar}), 6.66 (d, $J_{HH} = 8.1$ Hz, 1H; H_{ar}), 5.68–5.63 (m, 1H; CH_{allyl}), 4.97 (d, $J_{HH} = 17.4$, 1H; CH_{2allyl}), 4.65 (d, $J_{HH} = 10.2$ Hz, 1H; CH_{2allyl}), 3.54 (s, 3H; CH_3N), 3.52–3.38 ppm (m, 2H; CH_2P); $^{13}C\{^1H\}$ NMR ($CDCl_3$, 25°C): $\delta = 171.2$ (dd, $J_{CP} = 7.5$, 10.6 ppm; NCN), 137.8 (dd, $J_{CP} = 3.7$, 6.3 Hz; C_{ar}), 136.1 (s, C_{ar}), 136.0 (s, C_{ar}), 135.5 (dd, $J_{CP} = 5.3$, 7.5; CH_{ar}), 133.9 (dd, $J_{CP} = 4.5$, 7.4 Hz; CH_{ar}), 133.5 (s, C_{ar}), 132.8 (s, CH_{ar}), 132.3 (br s, CH_{ar}), 132.0 (dd, $J_{CP} = 4.5$, 7.1 Hz; CH_{ar}), 131.4 (s, CH_{ar}), 131.1 (dd, $J_{CP} = 2.7$, 4.8 Hz; CH_{ar}), 130.3–129.6 (m; C_{ar}), 129.6 (s, CH_{ar}), 129.5 (s, CH_{ar}), 129.4–129.1 (m; CH_{ar}), 129.0 (s, CH_{allyl}), 128.9–128.8 (m; CH_{ar}), 128.6 (dd, $J_{CP} = 3.3$, 6.7 Hz; CH_{ar}), 128.3 (d, $J_{CP} = 11.5$ Hz; CH_{ar}), 127.5 (dd, $J_{CP} = 1.6$, 3.5 Hz; C_{ar}) 127.4 (dd, $J_{CP} = 31.3$, 18.1 Hz; C_{ar}), 126.5 (br s, CH_{ar}), 125.5 (s, CH_{ar}), 125.1 (s, CH_{ar}), 125.0 (d, $J_{CP} = 53.8$ Hz; C_{ar}), 124.9 (d, $J_{CP} = 15.8$ Hz; C_{ar}), 122.8 (dd, $J_{CP} = 31.3$, 14.7 Hz; C_{ar}), 122.7 (s, CH_{ar}), 121.4–121.1 (m; CH_{allyl}), 121.0 (q, $J_{CF} = 321.0$ Hz; $CF_3SO_3^-$), 112.1 (s, CH_{ar}), 112.0 (s, CH_{ar}), 35.5 (s, CH_3N), 33.0 ppm (dd, $J_{CP} = 10.0$, 17.8; CH_2P); MS (ES^+): m/z: 809 $[M]^+$; HRMS (ES^+): m/z: calcd for $C_{45}H_{38}ClN_2P_2Pd$: 809.1234; found, 809.1270.

Compound 6: A mixture of tetraethylammonium chloride (0.094 g, 0.56 mmol) and BIMIONAP (**1**) (0.250 g, 0.32 mmol) was dissolved in CH_3CN (6 mL) and stirred at 50°C for 3 h. After evaporation of the solvent, the solid residue was purified by flash chromatography on silica gel (CH_2Cl_2/acetone) to afford **6** as a white powder. Yield: 0.126 g, 66%; m.p. 92–94°C; $^{31}P\{^1H\}$ NMR (CD_2Cl_2, 25°C): $\delta = -15.61$ ppm; ^1H NMR (CD_2Cl_2, 25°C): $\delta = 9.39$ (d, $J_{HP} = 1.8$ Hz, 1H; NCHN), 8.16 (d, $J_{HH} = 8.6$ Hz, 1H; H_{ar}), 8.09 (d, $J_{HH} = 8.2$ Hz, 1H; H_{ar}), 7.90 (d, $J_{HH} = 10.0$ Hz, 1H; H_{ar}), 7.73–7.68 (m, 2H; H_{ar}), 7.59–7.56 (m, 1H; H_{ar}), 7.49–7.42 (m, 4H; H_{ar}), 7.37 (d, $J_{HP} = 12.5$ Hz, 1H; H_{ar}), 7.34 (d, $J_{HP} = 3.2$ Hz, 1H; H_{ar}), 7.35–7.31 (m, 2H; H_{ar}), 7.28–7.25 (m, 3H; H_{ar}), 7.21–7.17 (m, 2H; H_{ar}), 6.89 (d, $J_{HH} = 8.5$ Hz, 1H; H_{ar}), 4.29 ppm (s, 3H, CH_3N); $^{13}C\{^1H\}$ NMR (CD_2Cl_2, 25°C): $\delta = 143.6$ (s, NCHN), 136.8 (d, $J_{CP} = 21.1$ Hz; C_{ar}), 134.4 (s, C_{ar}), 134.3 (d, $J_{CP} = 18.9$ Hz; C_{ar}), 134.2 (d, $J_{CP} = 22.0$ Hz; CH_{ar}), 133.8 (d, $J_{CP} = 20.5$ Hz; CH_{ar}), 133.6 (s, C_{ar}), 132.5 (s, C_{ar}), 131.9 (d, $J_{CP} = 22.8$ Hz; C_{ar}), 131.8 (s, CH_{ar}), 131.5 (s, C_{ar}), 129.9 (s, CH_{ar}), 129.8 (s, CH_{ar}), 129.7 (d, $J_{CP} = 2.1$ Hz; C_{ar}), 129.2 (s, CH_{ar}), 129.1 (d, $J_{CP} = 7.3$ Hz; CH_{ar}), 129.0 (s, CH_{ar}), 128.8 (d, $J_{CP} = 8.0$ Hz; CH_{ar}), 128.6 (s, CH_{ar}), 128.3 (s, CH_{ar}), 127.8 (s, CH_{ar}), 127.6 (s, CH_{ar}), 121.4 (d, $J_{CP} = 1.4$ Hz; CH_{ar}), 120.8 (q, $J_{CF} = 313.3$ Hz; $CF_3SO_3^-$), 113.8 (s, CH_{ar}), 113.1 (s, CH_{ar}), 34.1 ppm (s, CH_3N); MS (ES^+): m/z: 443 $[M]^+$; HRMS (ES^+): m/z: calcd for $C_{30}H_{24}N_2P$: 443.1677; found: 443.1686.

Compound 7: Butyllithium (2.5 M, 0.033 mL, 0.082 mmol) was added dropwise to a solution of BIMIONAP (**1**) (0.064 g, 0.082 mmol) in THF (3 mL) at −78°C and stirred for 20 min. Then a suspension of elemental sulphur S_8 (0.105 g, 0.41 mmol) in THF (3 mL) was added at −60°C to the solution. The mixture was slowly warmed to room temperature and stirring was continued for 3 h. After evaporation of the solvent, the solid residue was purified by chromatography on silica gel (CH_2Cl_2) to afford **7** as a white solid. Yield: 0.029 g, 71%; m.p. 268–270°C; $^{31}P\{^1H\}$ NMR ($CDCl_3$, 25°C): $\delta = +43.53$ ppm; ^1H NMR ($CDCl_3$, 25°C): $\delta = 8.14$–8.06 (m, 3H; H_{ar}), 7.99–7.92 (m, 2H; H_{ar}), 7.63–7.39 (m, 7H; H_{ar}), 7.27–7.11 (m, 3H; H_{ar}), 6.99 (d, $J_{HH} = 8.4$ Hz; 1H; H_{ar}), 6.92–6.83 (m, 4H; H_{ar}), 3.43 ppm (s, 3H; CH_3N); $^{13}C\{^1H\}$ NMR ($CDCl_3$, 25°C): $\delta = 170.7$ (s, CS), 135.6 (d, $J_{CP} = 2.2$ Hz; C_{ar}), 134.2 (d, $J_{CP} = 81.0$ Hz; C_{ar}), 133.9 (s, C_{ar}), 133.1 (d, $J_{CP} = 2.0$ Hz; C_{ar}), 133.0 (d, $J_{CP} = 87.8$ Hz; C_{ar}), 132.9 (d, $J_{CP} = 10.9$ Hz; CH_{ar}), 132.1 (d, $J_{CP} = 11.7$ Hz; CH_{ar}), 131.6 (d, $J_{CP} = 3.0$ Hz; CH_{ar}), 130.4 (d, $J_{CP} = 12.4$ Hz; CH_{ar}), 130.2 (d, $J_{CP} = 3.0$ Hz; CH_{ar}), 130.1 (s, CH_{ar}), 129.9 (d, $J_{CP} = 11.5$ Hz; CH_{ar}), 129.5 (d, $J_{CP} = 82.9$ Hz; C_{ar}), 128.7 (s, CH_{ar}), 128.5 (s, CH_{ar}), 128.3 (s, CH_{ar}), 128.2 (s, CH_{ar}), 128.1 (s, CH_{ar}), 126.3 (d, $J_{CP} = 13.1$ Hz; CH_{ar}), 123.6 (s, CH_{ar}), 123.4 (s, CH_{ar}), 111.0 (s, CH_{ar}), 108.5 (s, CH_{ar}), 30.6 ppm (s, CH_3N); MS (ES^+): m/z: 507 $[M+H]^+$; HRMS (ES^+): m/z: calcd for $C_{30}H_{24}N_2PS_2$: 507.1119; found: 507.1139 $[M+H]^+$; elemental analysis calcd (%) for $C_{30}H_{23}N_2PS_2 \cdot 0.9\,H_2O$: C 68.91, H 4.78, N 5.35; found: C 69.20, H 5.17, N 4.55.

Compound 8: Butyllithium (2.5 M, 0.04 mL, 0.1 mmol) was added dropwise to a solution of BIMIONAP (**1**) (0.081 g, 0.10 mmol) in THF (5 mL) at −78°C. Then the mixture was slowly warmed to room temperature and stirred for 3 h. After evaporation of the solvent, the solid residue was purified by chromatography on silica gel (CH_2Cl_2) to afford **8** as a white solid. Yield: 0.04 g, 87%; m.p. 228–230°C; $^{31}P\{^1H\}$ NMR ($CDCl_3$, 25°C): $\delta = -16.31$ ppm; ^1H NMR ($CDCl_3$, 25°C): $\delta = 8.28$ (s, 1H; CHO), 7.89 (d, $J_{HH} = 8.1$ Hz, 1H; H_{ar}), 7.79 (d, $J_{HH} = 8.1$ Hz, 1H; H_{ar}), 7.71 (d, $J_{HH} = 8.4$ Hz, 1H; H_{ar}), 7.56–7.51 (m, 1H; H_{ar}), 7.47–7.41 (m, 2H; H_{ar}), 7.40–7.28 (m, 9H; H_{ar}), 7.05 (d, $J_{HP} = 2.4$ Hz, 1H; H_{ar}), 7.02 (m, 1H; H_{ar}), 6.96–6.91 (m, 1H; H_{ar}), 6.77–6.72 (m, 1H; H_{ar}), 6.14 (d, $J_{HH} = 8.1$ Hz, 1H; H_{ar}), 5.87 (d, $J_{HP} = 1.8$ Hz, 1H; NH), 3.13 ppm (s, 3H; CH_3N); $^{13}C\{^1H\}$ NMR ($CDCl_3$, 25°C): $\delta = 163.7$ (s, CHO), 143.0 (s, C_{ar}), 139.8 (d, $J_{CP} = 21.6$ Hz; C_{ar}), 135.7 (d, $J_{CP} = 10.2$ Hz; C_{ar}), 134.8 (s, C_{ar}), 134.2–133.4 (br s, CH_{ar}), 132.4 (d, $J_{CP} = 10.1$ Hz; C_{ar}), 130.5 (d, $J_{CP} = 2.6$ Hz; C_{ar}), 129.5 (s, CH_{ar}), 129.3 (s, CH_{ar}), 129.2–128.5 (m; CH_{ar}), 128.3 (s, CH_{ar}), 128.2 (s, CH_{ar}), 127.4 (s, C_{ar}), 126.9 (s, CH_{ar}), 126.8 (s, CH_{ar}), 126.7 (s, CH_{ar}), 123.9 (d, $J_{CP} = 2.7$ Hz; CH_{ar}), 118.8 (s, CH_{ar}), 32.2 ppm (s, CH_3N); MS (ES^+): m/z: 461 $[M+H]^+$; HRMS (ES^+): m/z: calcd for $C_{30}H_{26}N_2OP$: 461.1783; found: 461.1793; elemental analysis calcd (%) for $C_{30}H_{25}N_2OP \cdot (C_4H_8O)$: C 76.67, H 6.25, N 5.26; found: C 76.85, H 6.27, N 4.90.

Computational details: Geometries of the model and fragments of BIMIONAP (**1**) were fully optimized at the (U)B3PW91/6–31G** level of calculation by using Gaussian 03.[46] Vibrational analysis was performed at the same level of calculation as the geometry optimization. AIM and ELF analyses of the experimental structures were performed with the TopMoD program[47] on the basis of the B3PW91/6–31G** wavefunction for free ligands (BIMIONAP and BIMINAP) and of the B3PW91/6–31G**/DGDZVP(Pd) one[46] for palladium complexes of BIMIONAP and BIMINAP. The gas-phase molecular electrostatic potential (MESP) was computed for the experimental geometries at the same level as above by using Gaussian 03.[46] The MESP has been shown to be weakly sensitive to the level of calculation.[48] Visualization of the isodensity surfaces colorcoded with the MESP were performed by using Molden.[49]

Crystal-structure determination of 3, 5, and 8: Intensity data for compounds **3**, **5**, and **8** were collected at 180 K on a Bruker Apex2 or an Xcalibur Oxford Diffraction diffractometer by using a graphite-monochromated $Mo_{K\alpha}$ radiation source and equipped with an Oxford Cryosystems Cryostream Cooler Device. Structures were solved by direct methods by using SIR92, and refined by full-matrix least-squares procedures on F by using the programs of the PC version of CRYSTALS. Atomic scattering factors were taken from the International tables for X-ray crystallography. All non-hydrogen atoms and nonsolvent molecules were refined anisotropically. Hydrogen atoms were refined by using a riding model. Absorption corrections were introduced by using the program MULTISCAN.

Crystal data for complex ***3***: $C_{30}H_{23}Cl_2N_2PPd$, CH_2Cl_2, $0.5\,CH_4O$, $0.17\,H_2O$; $M = 723.75\ g\,mol^{-1}$; trigonal; $a = 32.7191(3)$, $b = 32.7191(3)$, $c = 15.5065(4)$ Å; $V = 14376.3(4)$ Å^3; $T = 180$ K; space group $R-3$; $Z = 18$; $\mu(Mo_{K\alpha}) = 0.992\ mm^{-1}$; 133082 reflections measured, 13004 unique ($R_{int} = 0.02$), 10169 reflections used in the calculations [$I > 3\sigma(I)$], 356 parameters, $R1 = 0.0402$, $wR2 = 0.0450$.

Crystal data for complex ***5***: $C_{26}H_{26}N_2PPd$, CF_3O_3S, $M = 652.95\ g\,mol^{-1}$; triclinic; $a = 12.6140(3)$, $b = 12.2030(2)$, $c = 16.8654(7)$ Å; $\beta = 119.913(2)°$; $V = 2250.23(12)$ Å^3; $T = 180$ K; space group Pc; $Z = 2$; $\mu(Mo_{K\alpha}) = 0.765\ mm^{-1}$; 21663 reflections measured, 8732 unique ($R_{int} = 0.03$), 7596 reflections used in the calculations [$I > 3\sigma(I)$], 520 parameters, $R1 = 0.0548$, $wR2 = 0.0636$.

Crystal data for ***8***: $C_{30}H_{25}N_2OP$; $M = 460.52\ g\,mol^{-1}$; triclinic; $a = 9.8337(4)$, $b = 11.1319(4)$, $c = 11.6248(4)$ Å; $\alpha = 71.097(1)$, $\beta = 83.413(1)$, $\gamma = 85.522(2)°$; $V = 1194.83(8)$ Å^3; $T = 180$ K; space group $P-1$; $Z = 2$; $\mu(Mo_{K\alpha}) = 0.141\ mm^{-1}$; 26857 reflections measured, 7572 unique ($R_{int} = 0.02$), 5218 reflections used in the calculations [$I > 3\sigma(I)$], 307 parameters, $R1 = 0.0497$, $wR2 = 0.0556$.

Acknowledgements

The authors thank the french Ministère de l'Enseignement Supérieur et de la Recherche, the french Centre National de la Recherche Scientifique, and the Agence Nationale de la Recherche (program ANR-08-JCJC-0137-01) for financial support. The authors also thank the CALMIP (Calcul intensif en Midi-Pyrénées, Toulouse, France), the IDRIS (Institut du Développement et des Ressources en Informatique Scientifique, Orsay, France), and the CINES (Centre Informatique de l'Enseignement Supérieur, Montpellier, France) for computing facilities.

[1] If the dissociated fragments of the dative bond are neutral species M and L, the α-zwitterionic Lewis symbol M^-–L^+ is equivalent to the dative symbol M←L; a) R. S. Mulliken, W. B. Person, *Ann. Rev. Phys. Chem.* **1962**, *13*, 107; b) R. S. Mulliken, *J. Am. Chem. Soc.* **1952**, *74*, 811; c) A. Haaland, *Angew. Chem.* **1989**, *101*, 1017; *Angew. Chem. Int. Ed. Engl.* **1989**, *28*, 992; d) V. I. Minkin, *Pure Appl. Chem.* **1999**, *71*, 1933.

[2] a) E. M. Arnett, K. E. Molter, *Acc. Chem. Res.* **1985**, *18*, 339; b) S. Burck, K. Götz, M. Kaupp, M. Nieger, J. Weber, J. Schmedt auf der Günne, D. Gudat, *J. Am. Chem. Soc.* **2009**, *131*, 10763; c) Z. Benkó, S. Burck, D. Gudat, M. Hofmann, F. Lissner, L. Nyulászi, U. Zenneck, *Chem. Eur. J.* **2010**, *16*, 2857; d) C. A. Caputo, A. L. Brazeau, Z. Hynes, J. T. Price, H. M. Tuononen, N. D. Jones, *Organometallics* **2009**, *28*, 5261; e) D. Gudat, A. Haghverdi, H. Hupfer, M. Nieger, *Chem. Eur. J.* **2000**, *6*, 3414; f) N. Burford, P. J. Ragogna, *J. Chem. Soc. Dalton Trans.* **2002**, 4307.

[3] a) M. C. Jahnke, F. E. Hahn, *Top. Organomet. Chem.* **2010**, *30*, 95; b) S. Díez-González, N. Marion, S. P. Nolan, *Chem. Rev.* **2009**, *109*, 3612; c) F. E. Hahn, M. C. Jahnke, *Angew. Chem.* **2008**, *120*, 3166; *Angew. Chem. Int. Ed.* **2008**, *47*, 3122; d) D. Pugh, A. A. Danopoulos, *Coord. Chem. Rev.* **2007**, *251*, 610; e) S. P. Nolan, *N-Heterocyclic Carbenes in Synthesis*, Wiley-VCH, Weinheim, **2006**; f) N. Kuhn, A. Al-Sheikh, *Coord. Chem. Rev.* **2005**, *249*, 829; g) E. Peris, R. H. Crabtree, *Coord. Chem. Rev.* **2004**, *248*, 2239.

[4] Y. Wang, Y. Xie, P. Wei, R. B. King, H. F. Schaefer III, P. von R. Schleyer, G. H. Robinson, *Science* **2008**, *321*, 1069.

[5] A. Sidiropoulos, C. Jones, A. Stasch, S. Klein, G. Frenking, *Angew. Chem.* **2009**, *121*, 9881; *Angew. Chem. Int. Ed.* **2009**, *48*, 9701.

[6] Y. Wang, Y. Xie, P. Wei, R. B. King, H. F. Schaeffer III, P. von R. Schleyer, G. H. Robinson, *J. Am. Chem. Soc.* **2008**, *130*, 14970.

[7] a) O. Back, G. Kuchenbeiser, B. Donnadieu, G. Bertrand, *Angew. Chem.* **2009**, *121*, 5638; *Angew. Chem. Int. Ed.* **2009**, *48*, 5530; b) J. D. Masuda, W. W. Schoeller, B. Donnadieu, G. Bertrand, *J. Am. Chem. Soc.* **2007**, *129*, 14180; c) J. D. Masuda, W. W. Schoeller, B. Donnadieu, G. Bertrand, *Angew. Chem.* **2007**, *119*, 7182; *Angew. Chem. Int. Ed.* **2007**, *46*, 7052.

[8] a) C. A. Dyker, V. Lavallo, B. Donnadieu, G. Bertrand, *Angew. Chem.* **2008**, *120*, 3250; *Angew. Chem. Int. Ed.* **2008**, *47*, 3206; b) A. Fürstner, M. Alcarazo, R. Goddard, C. W. Lehmann, *Angew. Chem.* **2008**, *120*, 3254; *Angew. Chem. Int. Ed.* **2008**, *47*, 3210.

[9] a) P. A. Rupar, V. N. Staroverov, P. J. Ragogna, K. M. Baines, *J. Am. Chem. Soc.* **2007**, *129*, 15138; b) A. J. Ruddy, P. A. Rupar, K. J. Bladek, C. J. Allan, J. C. Avery, K. M. Baines, *Organometallics* **2010**, *29*, 1362.

[10] a) R. S. Ghadwal, H. W. Roesky, S. Merkel, J. Henn, D. Stalke, *Angew. Chem.* **2009**, *121*, 5793; *Angew. Chem. Int. Ed.* **2009**, *48*, 5683; b) A. C. Filippou, O. Chernov, G. Schnakenburg, *Angew. Chem.* **2009**, *121*, 5797; *Angew. Chem. Int. Ed.* **2009**, *48*, 5687.

[11] T. Matsumoto, F. P. Gabbaï, *Organometallics* **2009**, *28*, 4252.

[12] J. L. Dutton, H. M. Tuononen, P. J. Ragogna, *Angew. Chem.* **2009**, *121*, 4473; *Angew. Chem. Int. Ed.* **2009**, *48*, 4409.

[13] R. W. Alder, M. E. Blake, L. Chaker, J. N. Harvey, F. Paolini, J. Schütz, *Angew. Chem.* **2004**, *116*, 6020; *Angew. Chem. Int. Ed.* **2004**, *43*, 5896.

[14] a) A. H. Cowley, R. A. Kemp, *Chem. Rev.* **1985**, *85*, 367; b) D. Gudat, *Coord. Chem. Rev.* **1997**, *163*, 71; c) H. Nakazawa, *Adv. Organomet. Chem.* **2004**, *50*, 108; d) a cationic NHC–diaminophosphenium adduct has been prepared and characterized, see: N. J. Hardman, M. B. Abrams, M. A. Pribisko, T. M. Gilbert, R. L. Martin, G. J. Kubas, R. T. Baker, *Angew. Chem.* **2004**, *116*, 1989; *Angew. Chem. Int. Ed.* **2004**, *43*, 1955.

[15] a) C. W. Schultz, R. W. Parry, *Inorg. Chem.* **1976**, *15*, 3046; b) N. Burford, T. S. Cameron, P. J. Ragogna, *J. Am. Chem. Soc.* **2001**, *123*, 7947; c) N. Burford, P. J. Ragogna, R. McDonald, M. J. Ferguson, *J. Am. Chem. Soc.* **2003**, *125*, 14404.

[16] a) J. M. Slattery, C. Fish, M. Green, T. N. Hooper, J. C. Jeffery, R. J. Kilby, J. M. Lynam, J. E. McGrady, D. A. Pantazis, C. A. Russel, C. E. Willans, *Chem. Eur. J.* **2007**, *13*, 6967; b) N. Burford, D. E. Herbert, P. J. Ragogna, R. McDonald, M. J. Ferguson, *J. Am. Chem. Soc.* **2004**, *126*, 17067.

[17] B. D. Ellis, P. J. Ragogna, C. L. B. Macdonald, *Inorg. Chem.* **2004**, *43*, 7857.

[18] a) N. Debono, Y. Canac, C. Duhayon, R. Chauvin, *Eur. J. Inorg. Chem.* **2008**, 2991; b) M. Azouri, J. Andrieu, M. Picquet, H. Cattey, *Inorg. Chem.* **2009**, *48*, 1236; c) Y. Canac, N. Debono, L. Vendier, R. Chauvin, *Inorg. Chem.* **2009**, *48*, 5562.

[19] a) A. J. Arduengo III, C. J. Carmalt, J. A. C. Clyburne, A. H. Cowley, R. Pyati, *Chem. Commun.* **1997**, 981; b) N. Burford, T. S. Cameron, D. J. LeBlanc, P. Losier, S. Sereda, G. Wu, *Organometallics* **1997**, *16*, 4712.

[20] a) I. V. Komarov, M. Y. Kornilov, A. A. Tolmachev, A. A. Yurchenko, E. B. Rusanov, A. N. Chernega, *Tetrahedron* **1995**, *51*, 11271; b) N. Kuhn, J. Fahl, D. Bläser, R. Boese, *Z. Anorg. Allg. Chem.* **1999**, *625*, 729; c) N. Kuhn, M. Göhner, G. Henkel, *Z. Anorg. Allg. Chem.* **1999**, *625*, 1415; d) A. A. Tolmachev, A. A. Yurchenko, A. S. Merculov, M. G. Semenova, E. V. Zarudnitskii, V. V. Ivanov, A. M. Pinchuk, *Heteroat. Chem.* **1999**, *10*, 585.

[21] a) Y. Canac, R. Chauvin, *Eur. J. Inorg. Chem.* **2010**, 2325; b) S. Nanchen, A. Pfaltz, *Helv. Chim. Acta* **2006**, *89*, 1559; c) A. T. Normand, K. J. Cavell, *Eur. J. Inorg. Chem.* **2008**, 2781.

[22] CCDC-780614 (**3**), -780612 (**5**), and -780613 (**8**) contain the supplementary crystallographic data for this paper. These data can be obtained free of charge from The Cambridge Crystallographic Data Centre via www.ccdc.cam.ac.uk/data_request/cif.

[23] F. E. Hahn, M. C. Jahnke, T. Pape, *Organometallics* **2006**, *25*, 5927.

[24] I. Abdellah, N. Debono, Y. Canac, C. Duhayon, R. Chauvin, *Dalton Trans.* **2009**, 7196.

[25] a) S. A. MacGregor, *Chem. Soc. Rev.* **2007**, *36*, 67; b) R. Chauvin, *Eur. J. Inorg. Chem.* **2000**, 577.

[26] L. A. Evans, N. Fey, J. N. Harvey, D. Hose, G. C. Lloyd-Jones, P. Murray, A. G. Orpen, R. Osborne, G. J. J. Owen-Smith, M. Purdie, *J. Am. Chem. Soc.* **2008**, *130*, 14471.

[27] Instead of the expected ^{31}P NMR chemical shift of Ph_2PCl, two new signals at $\delta = +37.2$ (d) and -22.9 ppm (d), with $J_{PP} = 227.2$ Hz, were observed. They were attributed to $Ph_2PP(O)Ph_2$, which should result from a formal hydrolytic dimerization of Ph_2PCl, the exact mechanism of which under the present conditions has not been investigated.

[28] M. Yoshifuji, T. Ishizuka, Y. J. Choi, N. Inamoto, *Tetrahedron Lett.* **1984**, *25*, 553.

[29] G. A. Gray, S. E. Cremer, K. L. Marsi, *J. Am. Chem. Soc.* **1976**, *98*, 2109.

[30] Y. J. Bai, C. Y. Li, W. Sun, G. Zhao, Z. Shi, *Huaxue Shiji* **2008**, *30*, 409.

[31] a) Y. Canac, S. Conejero, M. Soleilhavoup, B. Donnadieu, G. Bertrand, *J. Am. Chem. Soc.* **2006**, *128*, 459; b) S. Conejero, M. Song, D. Martin, Y. Canac, M. Soleilhavoup, G. Bertrand, *Chem. Asian J.* **2006**, *1–2*, 155.

[32] a) A. D. Becke, K. E. Edgecombe, *J. Chem. Phys.* **1990**, *92*, 5379; b) B. Silvi, A. Savin, *Nature* **1994**, *371*, 683.

[33] R. F. W. Bader, *Atoms in Molecules*, Clarendon Press, Oxford, **1990**.

[34] a) C. Lepetit, B. Silvi, R. Chauvin, *J. Phys. Chem. A* **2003**, *107*, 464; b) B. Silvi, *Phys. Chem. Chem. Phys.* **2004**, *6*, 256.

[35] The valence populations are scaled to the actual number of electrons involved in the Lewis structures.

[36] a) A. Borgoo, D. J. Tozer, P. Geerling, F. De Proft, *Chem. Phys. Lett. Phys. Chem. Chem. Phys.* **2009**, *11*, 2862; b) A. Michalak, *Chem. Phys. Lett.* **2004**, *386*, 346.
[37] R. G. Parr, W. Yang, *J. Am. Chem. Soc.* **1984**, *106*, 4049.
[38] H. Chermette, P. Boulet, S. Portmann, *Rev. Mod. Quantum Chem.* **2002**, *2*, 992.
[39] F. A. Bulat, E. Chamorro, P. Fuentealba, A. Toro-Labbé, *J. Phys. Chem.* **2004**, *108*, 342.
[40] W. Tiznado, E. Chamorro, R. Contreras, P. Fuentealba, *J. Phys. Chem.* **2005**, *109*, 3220.
[41] a) C. Morell, A. Grand, A. Toro-Labbe, *J. Phys. Chem. A* **2005**, *109*, 205; b) C. Morell, A. Grand, S. Gutirrez-Oliva, A. Toro-Labbe, *Theor. Comput. Chem.* **2007**, *19*, 101; c) C. Cardenas, N. Rabi, P. W. Ayers, C. Morell, P. Jaramillo, P. Fuentealba, *J. Phys. Chem. A* **2009**, *113*, 8660.
[42] R. G. Pearson, *Inorg. Chem.* **1988**, *27*, 734.
[43] I. Abdellah, N. Debono, Y. Canac, L. Vendier, R. Chauvin, *Chem. Asian J.* **2010**, *5*, 1225.
[44] a) E. Sorocco, J. Tomasi, *Adv. Quantum Chem.* **1978**, *11*, 116; b) E. Sorocco, J. Tomasi in *Chemical Applications of Atomic and Molecular Electrostatic potentials* (Eds.: P. Politzer, D. G. Thruhlar), Plenum, New York, **1981**; c) P. Politzer, J. S. Murray, *Theor. Chem. Acc.* **2002**, 134.
[45] a) S. R. Gadre, S. A. Kulkarni, I. H. Shrivastava, *J. Chem. Phys.* **1992**, *96*, 5253; b) S. R. Gadre in *Computational Chemistry Reviews in Current Trends, Vol. 4* (Ed.: J. Leczynski), World Scientific, Singapore, **2000**, p. 1; c) S. R. Gadre, R. N. Shirsat in *Electrostatics of Atoms and Molecules*, Universities Press, Hyderabad, **2000**.
[46] Gaussian 03, Revision C.02, M. J. Frisch, G. W. Trucks, H. B. Schlegel, G. E. Scuseria, M. A. Robb, J. R. Cheeseman, J. A. Montgomery, Jr., T. Vreven, K. N. Kudin, J. C. Burant, J. M. Millam, S. S. Iyengar, J. Tomasi, V. Barone, B. Mennucci, M. Cossi, G. Scalmani, N. Rega, G. A. Petersson, H. Nakatsuji, M. Hada, M. Ehara, K. Toyota, R. Fukuda, J. Hasegawa, M. Ishida, T. Nakajima, Y. Honda, O. Kitao, H. Nakai, M. Klene, X. Li, J. E. Knox, H. P. Hratchian, J. B. Cross, C. Adamo, J. Jaramillo, R. Gomperts, R. E. Stratmann, O. Yazyev, A. J. Austin, R. Cammi, C. Pomelli, J. W. Ochterski, P. Y. Ayala, K. Morokuma, G. A. Voth, P. Salvador, J. J. Dannenberg, V. G. Zakrzewski, S. Dapprich, A. D. Daniels, M. C. Strain, O. Farkas, D. K. Malick, A. D. Rabuck, K. Raghavachari, J. B. Foresman, J. V. Ortiz, Q. Cui, A. G. Baboul, S. Clifford, J. Cioslowski, B. B. Stefanov, G. Liu, A. Liashenko, P. Piskorz, I. Komaromi, R. L. Martin, D. J. Fox, T. Keith, M. A. Al-Laham, C. Y. Peng, A. Nanayakkara, M. Challacombe, P. M. W. Gill, B. Johnson, W. Chen, M. W. Wong, C. Gonzalez, J. A. Pople, Gaussian, Inc., Wallingford CT, **2004**.
[47] S. Noury, X. Krokidis, F. Fuster, B. Silvi, *Comput. Chem. Eng.* **1999**, *23*, 597.
[48] S. A. Kulkarni, S. R. Gadre, *Chem. Phys. Lett.* **1997**, *274*, 255.
[49] Molden software, G. Schaftenaar, CMBI: http://www.cmbi.ru.nl/molden/molden.html.

Received: June 17, 2010
Published online: September 24, 2010

